ISSN 0869-5911, Petrology, 2024, Vol. 32, No. 2, pp. 179–200. © Pleiades Publishing, Ltd., 2024.

Model of the Formation of Monzogabbrodiorite–Syenite–Granitoid Intrusions by the Example of the Akzhailau Massif (Eastern Kazakhstan)

P. D. Kotler[a, b, *], S. V. Khromykh[a], A. V. Zakharova[b], D. V. Semenova[a, c], A. V. Kulikova[a, c], A. G. Badretdinov[c], E. I. Mikheev[a, b], and A. S. Volosov[a, b]

[a] *V.S. Sobolev Institute of Geology and Mineralogy, Siberian Branch, Russian Academy of Sciences, Novosibirsk, Russia*

[b] *Novosibirsk State University, Novosibirsk, Russia*

[c] *Kazan Federal University, Kazan, Russia*

**e-mail: pkotler@yandex.ru*

Received August 21, 2023; revised September 14, 2023; accepted October 19, 2023

Abstract—This paper presents a model of the formation of a multiphase Akzhailau granitoid massif formed within a Caledonian block of the Earth's crust in the Hercynian time. This work is based on the results of major and trace element composition, geochronological, mineralogical and isotope-geochemical studies. Three stages of the formation of the Akzhailau massif are distinguished, which differ significantly from the previously accepted concepts about the multicomplex and polychronous origin of this intrusion: (1) the formation of moderately alkaline A_2-type leucogranites (308–301 Ma); (2) intrusion of monzodiorites into the base of leucogranites (~295 Ma), increasing degree of partial melting of protoliths with the formation of syenites and moderately alkaline granites of I-type (294–292 Ma); (3) intrusion of dikes and small bodies of alkaline ferroeckermannite A_1-type leucogranites in the west and north of massif (~289 Ma). The Akzhailau massif was formed within about 15 Myr in the middle–upper crust through the interaction of plume-related subalkaline basitic magmas with metamorphosed crustal protolith of the orogenic structure.

Keywords: granitoids, multiple-phase intrusions, mantle-crust interaction, Eastern Kazakhstan, Central Asia

DOI: 10.1134/S086959112402005X

INTRODUCTION

In spite of a large empirical dataset on granitoids (Frost et al., 2001; Rosen and Fedorovsky, 2001; Frost and Frost, 2011; Grebennikov, 2014; Yarmolyuk et al., 2016a, etc.) and significant progress in experimental studies in this field (Beard and Lofgren, 1991; Vielzeuf and Montel, 1994; Patiño Douce, 1999, etc.), a common approach to the explanation of genesis and geochemical diversity of these rocks has not been developed yet. There is no consensus concerning the composition of primary magmas, duration of the emplacement and formation of the massif, possible ways of differentiation of granitoid melts, and their metallogenic specialization.

The study of intricate pluton consisting of geochemically different intrusive phases allows deciphering the genesis of granitoid magmas. According to the traditional concepts based, first of all, on the geological relations of rocks of different types, such plutons were ascribed to the polychronous formations with long-term evolution (D'yachkov, 1972; Ermolov et al., 1977, 1983; Lopatnikov et al., 1982, and others). At the same time, owing to the wide development of isotope-geochronological studies, more and more data point to the subsimultaneous formation of geochemically diverse intrusive rocks (Tsygankov et al., 2016; Khubanov et al., 2016; Khromykh et al., 2016; Yarmolyuk et al., 2016b; Kotler et al., 2021, and others), which demonstrates complex magma generation mechanisms in the Earth's crust likely from different sources and a possible contribution of mantle-derived magmas. Thereby, in order to develop the petrogenetic models, it is important to decipher the mechanisms of magma generation, their interactions and differentiation based on the detailed study of geological relations of rocks, petrography, mineralogy, chemical and isotope composition.

This approach was applied by us to the rocks of the Akzhailau massif, which is located in the junction zone of the Hercynian Ob–Zaisan and Caledonian Chingiz–Tarbagatai orogenic systems. This massif has been studied for a long time (Ermolaev et al., 1977; Beskin et al., 1979 and references therein), which is caused by the diversity of types of intrusive granites, the wide development of fields and areas of rock crystal-bearing granite pegmatites, and, the occurrence of the leucogranite-related Verkhnee Espe rare-metal–

rare-earth deposit in the northeastern part of the massif (Frolova, 2018; Levashova et al., 2022). In spite of the great body of accumulated data on the geological structure, petrography, and mineralogy of massif rocks, the modern analytical facilities practically were not applied during its study. This work presents new petrological model of the formation of rocks of this massif based on the results of modern geochronological, mineralogical, and isotope-geochemical investigations.

GEOLOGICAL BACKGROUND

The test site is localized in the western part of the Central Asian Orogenic Belt and ascribed to the Hercynian Ob–Zaisan (Irtysh–Zaisan) orogenic area (Fig. 1). The Akzhailau massif is located in the western part of the Zharma–Saur zone, which represented an active margin of the Ob-Zaisan Ocean (in the west in the present-day coordinates) in the Middle–Late Paleozoic. The eastern part of the Zharma–Saur zone contains mainly Late Paleozoic volcanic rocks representing fragments of Late Devonian–Early Carboniferous island arc. The western part of the zone contains mainly terrigenous sedimentary sequences, which, according to (Degtyarev, 2012), were formed in a back-arc trough on the Caledonian basement. In the Akzhailau pluton area, the terrigenous sediments of the Visean Kokna Formation (sandstones and siltstones) are exposed at the present-day erosion surface. The end of Early Carboniferous (Serpukhovian) is marked by the closure of the Ob-Zaisan oceanic basin and convergence of the Kazakhstan and Siberian continents. The age of the collisional event is estimated as the Early–Middle Carboniferous boundary (Zonenshain et al., 1990; Vladimirov et al., 2008). The collapse of the orogenic build-up occurred in the Late Carboniferous, while the Early Permian post-collisional stage produced large-scale magmatism (first of all, granitoid), which is thought to be related to the lithosphere extension against the background of thermal anomaly caused by the activity of the Tarim mantle plume (Khromykh et al., 2019; Khromykh, 2022).

Detailed geological studies of the intrusive magmatism of the Zharma–Saur zone were carried out in 1960–1970s (Shcherba et al., 1976; Ermolov et al., 1977). The diversity of intrusive rocks of the Zharma–Saur zone differing in the textural–structural features, mineral and chemical composition served as the basis for the recognition of several gabbroid, gabbro-granitoid, and granitoid series, complexes, and volcanoplutonic associations. Based on the relations between different intrusive phases, the plutonic magmatism lasted from the Early Carboniferous to the Late Permian–Triassic.

FACTUAL MATERIAL AND METHODS

This work is based on author's collection consisting of 58 samples collected during field works.

Petrographic studies (25 polished thin sections) were carried out using Carl Zeiss Axio Lab polarization microscope at the Institute of Geology and Mineralogy of the Siberian Branch of the Russian Academy of Sciences (IGM, SB RAS, Novosibirsk). Photos of polished thin sections were acquired using Canon PowerShot A 590 digital camera appended to microscope.

Major oxides were analyzed at the IGM SB RAS by the X-ray fluorescence in fused tablets of rock samples on an Applied Research Laboratories ARL-9900-XP spectrometer (analyst N.G. Karmanova). The rare-element composition of rocks was measured by ICP-MS on an Finnigan Element II mass spectrometer following technique described in (Nikolaeva et al., 2012).

The compositions of amphiboles and feldspars (800 determinations) were analyzed at the IGM SB RAS by energy dispersive spectroscopy using a Tescan MIRA 3LMU scanning electron microscope equipped with an Aztech microprobe system (Oxford Instruments Nanoanalysis Ltd., analyst M.V. Khlestov). Obtained data were processed in Microsoft Excel. Minerals were classified using works (Leake et al., 1997; Rieder et al., 1998). Biotite composition was analyzed on an JXA-8100 (Jeol Ltd.) microprobe (Center for Collective Use of Multielement and Isotope Studies, SB RAS, Novosibirsk, analyst V.N. Korolyuk) at an accelerated voltage of 20 kV, a beam current of 40 nA, a counting time of 10 s (for all elements, except for fluorine) and 30 s (for fluorine), and a diameter of analyzed area of 2 μm. After each tenth measurement, the following standards were analyzed to monitor the measurement accuracy: BD (diopside, measurement of SiO_2, MgO, CaO), 359-1 (orthoclase, Al_2O_3 measurement), albite (Na_2O), O-145 and IGEM (garnets, measurement of FeO and MnO, respectively), F-flog and Cl-flog (phlogopites, measurement of F and Cl, respectively), and Gl-6 (synthetic glass, measurement of TiO_2).

U-Pb zircon dating was performed at the Analytical Center of Multielement and Isotope Studies of the Institute of Geology and Mineralogy of the Siberian Branch, Russian Academy of Sciences (AC MIS, IGM SB RAS, Novosibirsk), analyst D.V. Semenova. Dating points were selected using cathodoluminescence images obtained on a LEO-1430VP scanning electron microscope. Concentrations of U, Th, and Pb isotopes were measured on a high-resolution inductively coupled plasma Thermo Scientific Element XR (Thermo Fisher Scientific, Germany) mass spectrometer coupled with UP 213 laser ablation system (New Wave Research, USA), following technique described in (Khubanov et al., 2016). The analyses were conducted using 25 μm or 30 μm laser beam diameter, 5 Hz frequency, and energy density of ~3 J/cm^2. Mass spectrometric data were processed using Glitter software (Griffin et al., 2008). U-Pb isotope ratios were normalized to the corresponding values of isotope ratios of standard zircons TEMORA-2 (Black et al., 2004)

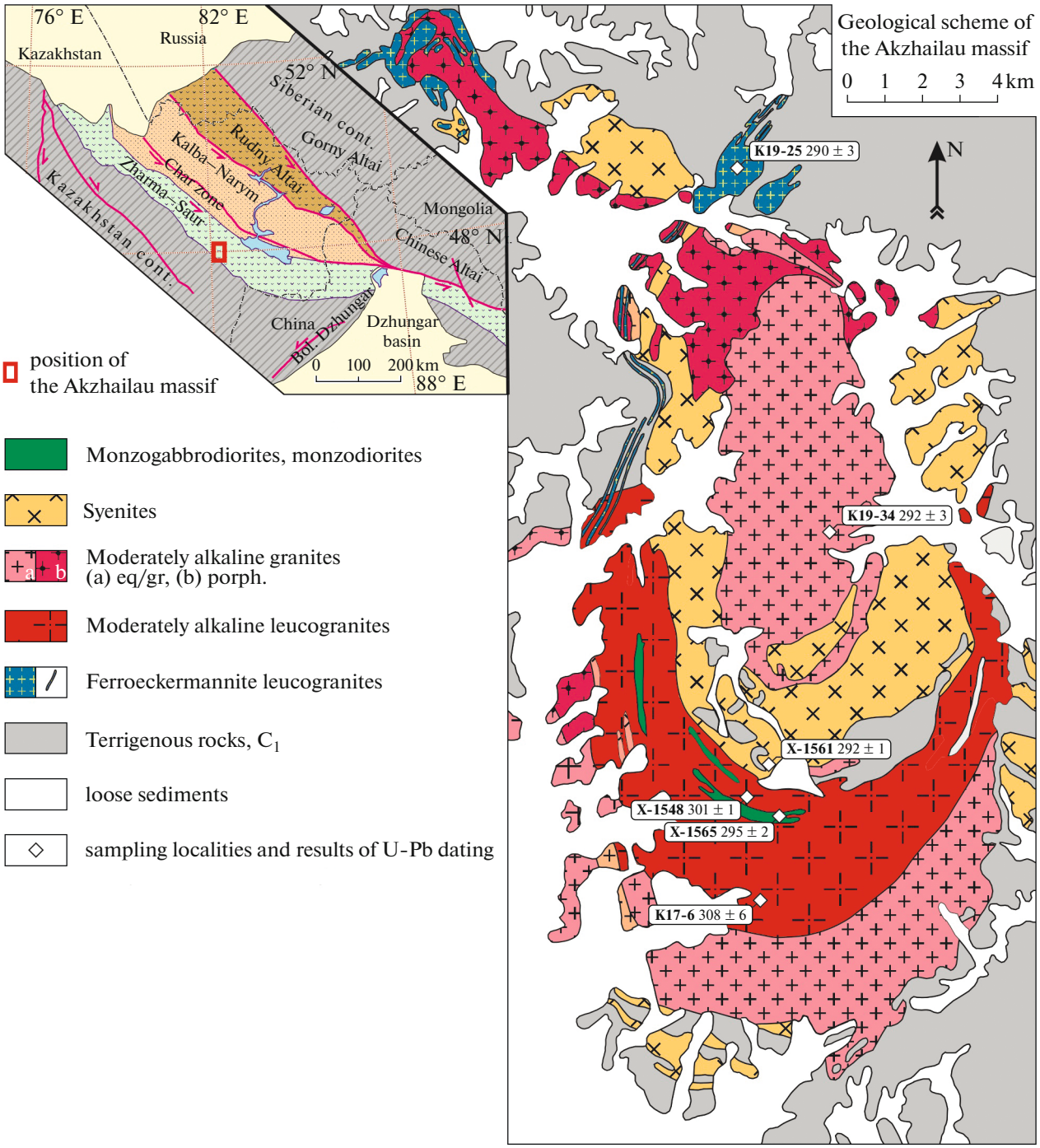

Fig. 1. Geological scheme of the Akzhailau massif. Inset shows the position of the Akzhailau massif in the structures of the Ob-Zaisan orogenic system after (Khromykh et al., 2019).

and Plešovice (Slama et al., 2008). The errors of single measurements (ratios, ages) were at 1σ levels, and the errors of calculated concordant ages were at 2σ level. Ages were calculated by consideration of U-Pb ($^{206}Pb/^{238}U$–$^{207}Pb/^{235}U$) system in concordia. Concordia diagrams were plotted using Isoplot program (Ludwig, 2003). In addition, one sample was dated using Analyte Excite (Teledyne Cetac Technologies) excimer laser ablation system (wave length of 193 nm) coupled with ThermoScientific iCAP Q quadrupole mass spectrometer with inductively coupled plasma ionization in Research–Educational Center of Geothermochronology of the Institute of Geology and Petroleum Technologies, Kazan Federal University.

Ar-Ar isotope dating was carried out at the Analytical Center of the Multielement and Isotope Studies of

SB RAS (Novosibirsk) in aliquots of amphibole monofractions by stepped heating following technique (Travin et al., 2009). Monomineral fractions for studies were hand-picked under microscope from 0.5–0.25 mm fraction after rock brecciation and magnetic separation. Samples of mineral fractions were wrapped in aluminum foil and after evacuation were sealed in a quartz capsule together with samples of biotite MCA-11 and LP-6, muscovite Bern 4m as monitors. Then samples were irradiated in Cd channel of VVR-K type research reactor at the Research Nuclear Reactor, Tomsk Polytechnical University. Gradient of the neutron flux was no more than 0.5% over sample area. After pause required to decrease radioactivity, samples were delivered to the IGM SB RAS for measurements. Experiments on stepped heating of samples were conducted in a quartz reactor with an external heating furnace. Blank for ^{40}Ar at 1200°C during 10 min was no more than 5×10^{-10} cm^3. Argon was purified using Ti- and ZrAl SAES getters. The Ar isotopic composition was measured on a Noble Gas 5400 Micromass mass spectrometer, UK. Measurement error corresponds to $\pm 1\sigma$.

The Sm and Nd concentrations and isotope composition were measured at the Geoanalitik Center for Collective Use (Institute of Geology and Geochemistry, Ural Branch, Russian Academy of Sciences, Yekaterinburg). The procedure of chemical preparation of samples involved the decomposition of samples in a mixture of mineral acids (at 120°C) with addition of isotope spike ^{149}Sm–^{150}Nd, chromatographic separation of total REE and stepwise separation of Sm and Nd. Isotope ratios were measured by TIMS on a Thermo Finnigan Triton Plus spectrometer in a static mode. The quality of the measurements was controlled using isotope standard JNd_i-1 (GSJ). The $^{143}Nd/^{144}Nd$ value in standard during the measurements was 0.512111 ± 9 (2 SD, $N = 7$). Rb-Sr whole rock isotope studies were carried out on a solid-phase MI-1201-AT mass spectrometer at the Institute of Geology and Mineralogy, Siberian Branch, Russian Academy of Sciences. Initial Sr isotope ratios were calculated using the decay constants of ^{87}Rb equal 1.42×10^{-11} yr^{-1} (Steager and Jäger, 1977).

RESULTS

Geological Position, Perography, and Mineralogy

At the present-day erosion surface, the Akzhailau massif has a sublongitudinal oval shape widening to the south, over 35 km long at a width from 10 to 20 km. Based on geophysical data (Ermolov et al., 1977), the present-day shape of the Akzhailau massif is determined by a combination of two bodies: asymmetric low-angle ethmolith with a steep magma conduit channel in the central part of the massif and arched garpolith conical in section in the southern part of the massif. According to the early studies of the geological relations and petrography of rocks, the pluton is subdivided into three magmatic complexes, which rocks were formed during 11 intrusive phases (Ermolov et al., 1977). The Permian age of the complexes of the massif was accepted conditionally on the basis of geological relations (the granites cut across the Carbonaceous sedimentary rocks) and mean K-Ar ages. Previous researchers believed that the massif was formed in a basic to acid sequence. Previous researchers believe that the massif was formed in basic to acid sequence. The early phase included gabbroids, granosyenites, and granites united into the Zharma Series (P_1). The second phase was related to the alkaline granites and granite porphyries of the Keregetas–Espe Complex (P_2), while phases made up of medium to coarse grained leucogranites were considered as the latest and were ascribed to the Late Permian Karakol Complex.

The petrographic, mineralogical, major-, trace-element and isotope-geochemical studies as well as results of U-Pb isotope dating allowed us to distinguish five groups of intrusive rocks corresponding to the intrusive phases (Fig. 1): (1) monzogabbrodiorites and monzodiorites, (2) syenites, (3) moderately alkaline granites, (4) moderately alkaline leucogranites, and (5) ferroeckermannite leucogranites.

The monzogabbrodiorites and monzodiorites occur as small extended lenticular bodies in the central part of the massif among the leucogranites. Previously, these bodies were described as remnants and xenoblocks in leucogranite, which are conformable to the main ring plan of the intrusion and gently plunge in the northern direction (Ermolov et al., 1977). The bodies are poorly exposed, usually composing the lowering in the topography. The most representative exposures are situated at the base of leucogranite cliffs where we managed to document contacts between the rocks. The contact of the monzodiorites with granitoids is uneven scalloped (festoon), with traces of mutual penetration of xenoliths (Fig. 2), which indicates the interaction of basite magma with felsic magma or with weakly consolidated granitoids (Renna et al., 2006; Burmakina and Tsygankov, 2013).

The predominant rocks of this group are medium-grained hornblende–biotite monzodiorites (Fig. 3) made up of up to 60 vol % plagioclase (*An* 26–57), 5–20 vol % K-feldspar, up to 5 vol % interstitial quartz, 15–45 vol % brownish-green hornblende (Fig. 4), <1–10 vol % brown biotite, and scarce single grains of diopside–augite. Accessory minerals are apatite, titanite, zircon, ilmenite, Ti and V-bearing magnetite, epidote, and rutile.

Syenites compose the marginal parts of the low-angle cup-shaped intrusion (ethmolith) in the central part of the Akzhailau massif. At the studied areas of the massif, the contacts of the syenites with granitoids are turfed. The rocks are represented by leucocratic biotite syenites consisting of 45–70 vol % microcline-perthite, 10–25 vol % sodic plagioclase (*An* 2–12), 5–

Fig. 2. Exposures of the rocks of the Akzhailau massif; mingling—contacts between leucogranites and monzogabbrodiorites.

15 vol % quartz, up to 15 vol % biotite, and up to 5 vol % amphibole (ferroedenite) (Fig. 4). Accessory minerals are Ce-bearing apatite, titanite, zircon, ilmenite, V-bearing magnetite, and monazite.

Moderately-alkaline granites occupy significant areas at the present-day erosion surface of the Akzhailau massif and are represented by equigranular and porphyritic varieties. According to (Ermolov et al., 1977), the equigranular granites compose the main volume of asymmetric ethmolith in the central part of the massif, representing a regular ellipse at a present-day erosion surface. The porphyritic granites compose a relatively narrow linear NW-trending body in the northern part of the massif, which is extended parallel to strikes of fault structures bounding the Zharma–Saur zone. The medium-grained granites are composed of 40–50 vol % microcline perthite, 15–25 vol % quartz, 20–25 vol % plagioclase, 5–10 vol % biotite, and up to 1 vol % amphibole. Fine-grained granites consist of 35–40 vol % microcline perthite, 35–40 vol % plagioclase (*An* 4–7), 25–30 vol % quartz, 3–5 vol % biotite, and <1 vol % muscovite in single samples. The porphyritic granites have medium to fine-grained texture of groundmass, while phenocrysts are represented by microcline perthite. The groundmass consists of 45–50 vol % microcline-pertite, 25–30 vol % quartz, 15–20 vol % plagioclase, 2–5 vol % biotite, and sporadic amphibole (up to 1%). Accessory minerals in all varieties are zircon, titanite, rutile, and ilmenite.

Moderately alkaline leucogranites are restricted mainly to the southern part of the massif, form crescent-shaped body in a plan view and conical in section. The leucogranites are well expressed in topography as large rocky crests. Convex-upward side of the arc is faced to the south, at a maximum width of ~4 km and a width at a closure of ~1.5 km. The dip is gentle with a slope angle of 30° to the north. It should be noted that the central part of the crescent-type body comprises significant part of pegmatite bodies, which were mined in the Soviet time for rock crystal. This group includes several varieties. Porphyritic leucogranites contain large phenocrysts of K-feldspar (from 15 to 40 vol %) and fine to medium-grained groundmass. The groundmass consists of 25–30 vol % quartz, up to 3 vol % biotite, and single grains of amphibole represented by edenite. Micas in the moderately alkaline leucogranites are low-Mg with moderate to elevated content of Ti and Al and in composition occupy an intermediate position between siderophyllite and Fe-rich muscovite. Equigranular leucogranites consist of 40–50 vol % microcline perthite, 10–25 vol % plagioclase, 25–40 vol % quartz, and<1–3 vol % biotite. Accessory minerals are titanite, zircon, ilmenite, ilmenorutile, and F-bearing oxide of cerium, lanthanum, thorium, and neodymium, as well as bastnaesite and rutile.

Ferroeckermannite leucogranites form a dike belt cutting across moderately alkaline granites in the western part of the massif, as well as three intrusive stocks in the northern part of the Akzhailau pluton up to 3 km^2 in size (Bol'shoi and Malyi Espe in the northeast and Iisor in the northwest). The ferroeckermannite leucogranite bodies are restricted to the contact planes of bodies of moderately alkaline granites with host sandy-shaly sequences, as well as to the network of differently oriented fractures and faults cutting across granitoids of previous phases of the massif. These rocks are mainly represented by medium-grained equigranular or porphyritic leucocratic granites. Two rock varieties are distinguished: ferroeckermannite (Bol'shoi and Malyi Espe stocks) and ferroeckermannite–arfvedsonite leucogranites (Iisor massif). The rocks are made up of the following minerals (in vol %): 30–60 microcline perthite, 35–50 quartz, 10–30 albite, 3–10 ferroeckermannite, 0–5 arfvedsonite, and <1 aegirine. Accessory minerals are F-bearing oxides of cerium, lanthanum, praseodymium, and neodymium, Nb-bearing hematite, and thorium oxide.

Composition

Composition of all rock varieties are presented in Table 1.

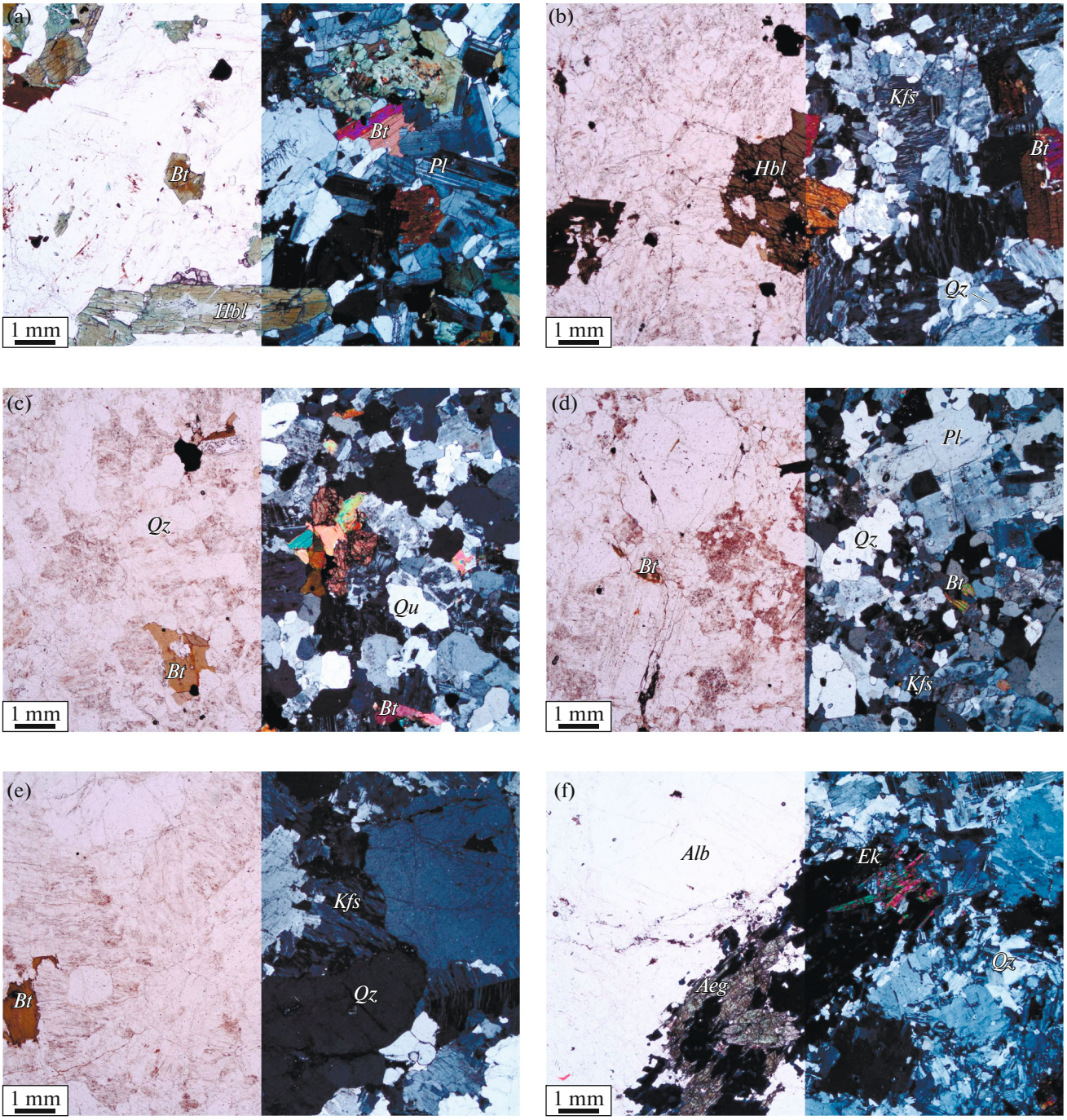

Fig. 3. Photos of polished thin sections of the Akzhailau massif rocks (left side—in transmitted light, right side—in crossed nicols): (a) monzogabbrodiorite, (b) syenite, (c) equigranular granite, (d) porphyritic granite, (e) leucogranite, (f) ferroeckermannite leucogranite. (*Bt*) biotite, (*Pl*) plagioclase, (*Hbl*) hornblende, (*Kfs*) K-feldspar, (*Qz*) quartz, (*Ab*) albite, (*Eck*) eckermannite, (*Aeg*) aegirine.

Monzogabbrodiorites and monzodiorites. These rocks have the following composition (in wt %): SiO_2 51.9–55.9, CaO 6.12–7.9; Al_2O_3 16.6–17.9; TiO_2 1.34–1.47, $(Na_2O + K_2O) = 5.6–7.11$ with $K_2O/Na_2O = 0.26–0.61$ (Fig. 5); femic components ($FeO + Fe_2O_3 + MgO$) = 11.6–14.1 wt % with $FeO^*/(FeO^* + MgO) = 0.66–0.7$. In the TAS-diagram (Sharpenok et al., 2013), data points of these rocks plot in the fields of monzogabbrodiorites and monzodiorites. According to the diagram $SiO_2–K_2O$ (Rickwood, 1989), the monzogabbrodiorites and monzodiorites are ascribed to the calc-alkaline and high-K calc-alkaline series. The REE patterns of the rocks (Fig. 6) show LREE

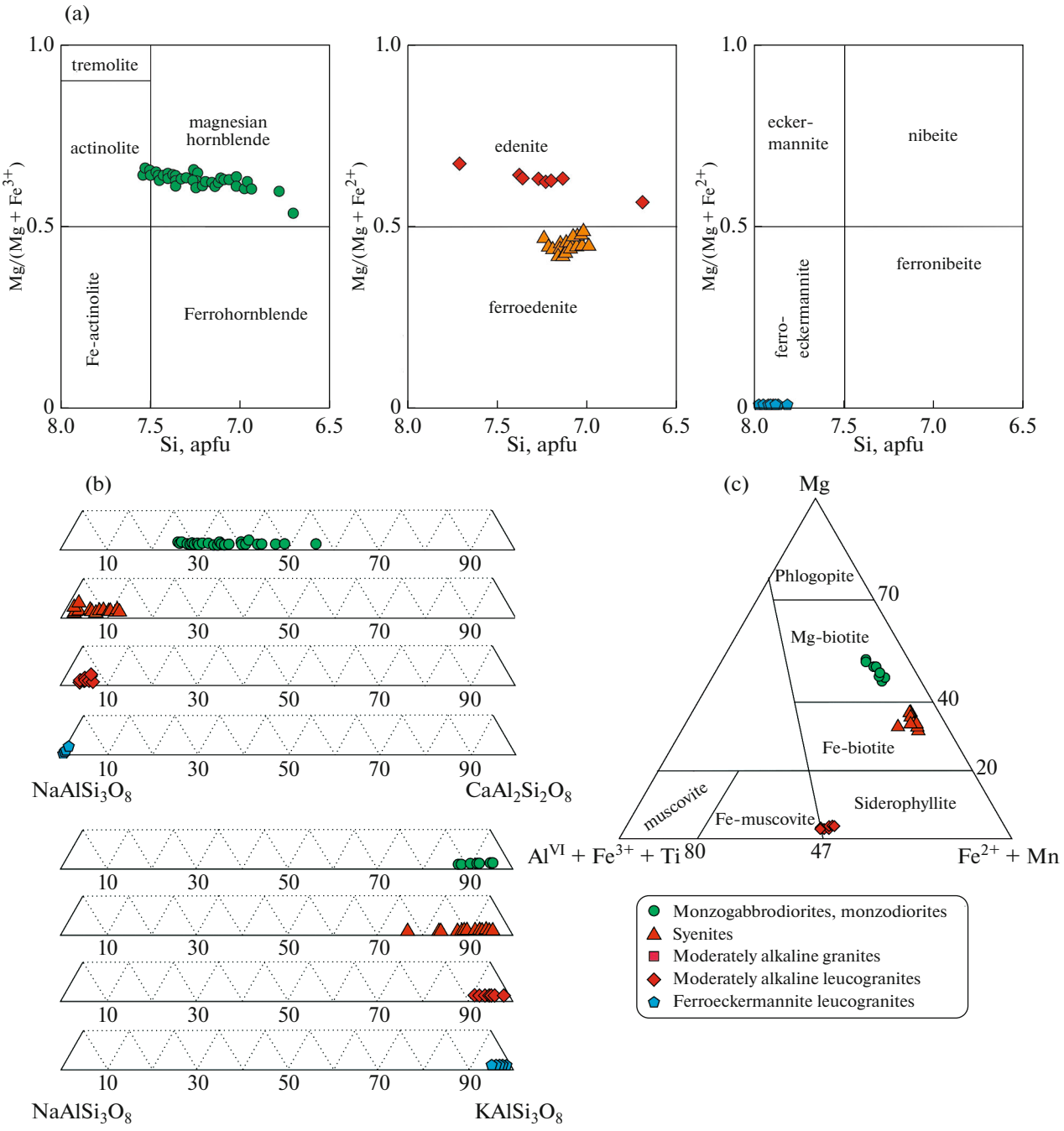

Fig. 4. Composition of rock-forming minerals in the rocks of the Akzhailau massif: (a) compositions of amphiboles, classification after (Leake et al., 1997); (b) composition of plagioclases (top) and feldspars (down); (c) composition of micas.

predominance over HREE, a weakly expressed negative Eu anomaly (Eu/Eu*) = 0.83–0.88, La_n/Yb_n = 8.2–8.83, and total REE of 194–268 ppm. The multielement patterns show a negative Ti anomaly and a positive Sr anomaly.

Syenites contain (in wt %): SiO_2 62.9–65.5, CaO 1.48–2.4, Al_2O_3 15.8–17.9, TiO_2 0.78–0.83, (Na_2O + K_2O) = 9.3–11.4 with K_2O/Na_2O = 0.74–1.06; femic components (FeO + Fe_2O_3 + MgO) = 4.32–5.25 wt % with FeO*/(FeO* + MgO) = 0.79–0.89. In the TAS-diagram (Sharpenok et al., 2013) (Fig. 6), data points of these rocks are localized in the composition fields of syenites and granosyenites and are ascribed to the shoshonite and high-K calc-alkaline series, according to the SiO_2–K_2O diagram. In the REE pattern, LREE predominates over HREE, Eu anomaly is practically absent (Eu/Eu*) = 0.74–0.96, except for sample X-1561 with a positive Eu anomaly (2.13),

Table 1. Composition of rocks of representative samples of the Akzhailau massif

Components	Monzogabbrodiorites				Syenites			Moderately-alkaline granites			
	X-1549	X-1553	X-1556	X-1557	X-1545	X-1561	K17-13	X-1550	K19-34	K1936	K19-37
SiO_2	52.11	53.60	55.60	54.49	63.08	62.84	65.13	72.69	73.12	71.86	72.27
TiO_2	1.36	1.38	1.34	1.35	0.78	0.78	0.83	0.37	0.16	0.26	0.27
Al_2O_3	17.59	17.23	16.56	16.81	17.35	17.90	15.69	13.64	13.97	14.23	14.23
$Fe_2O_3^*$	9.51	8.82	8.01	8.29	4.50	3.72	4.16	2.11	1.51	2.07	2.12
MnO	0.17	0.15	0.14	0.17	0.12	0.10	0.11	0.04	0.03	0.07	0.08
MgO	4.12	4.21	3.55	3.88	0.56	0.59	1.06	0.38	0.24	0.39	0.42
CaO	7.28	7.28	6.10	6.57	1.62	1.47	2.39	0.95	1.07	1.08	1.17
Na_2O	4.36	4.74	4.39	5.01	5.54	5.53	5.33	3.94	3.38	3.69	3.78
K_2O	1.84	1.21	2.69	1.31	5.56	5.83	3.92	4.74	5.01	4.68	4.68
P_2O_5	0.50	0.51	0.51	0.54	0.14	0.12	0.24	0.09	0.05	0.08	0.08
L.O.I.	0.45	0.64	0.53	0.54	0.15	0.37	0.38	0.21	0.51	0.57	0.46
Total	99.51	99.98	99.62	99.12	99.72	99.80	99.43	99.30	99.23	99.17	99.73
Rb	25	25	66	34	72	52	79	115	177	161	159
Sr	736	695	663	581	194	212	353	135	210	197	206
Y	47	29	31	26	30	21	36	31	13.0	21	18.9
Zr	330	261	299	283	887	888	373	276	127	192	205
Nb	25	24	27	24	37	23	36	38	21	23	24
Cs	0.50	0.89	1.44	0.89	0.66	0.48	3.9	1.48	3.0	3.3	3.1
Ba	996	792	864	536	1864	3591	982	549	1050	962	939
La	51	46	51	44	47	30	52	53	32	57	45
Ce	104	92	97	87	91	57	101	100	49	80	77
Pr	13.6	10.5	11.5	10.4	10.5	7.0	11.4	10.9	5.0	10.2	8.2
Nd	53	40	42	39	42	27	41	36	15.4	33	27
Sm	10.6	7.2	7.7	7.1	7.5	5.0	7.7	6.2	2.6	5.2	4.3
Eu	2.9	2.00	2.00	1.89	2.3	3.3	1.76	0.99	0.49	0.92	0.86
Gd	10.5	6.7	7.0	6.3	7.0	4.4	6.9	5.5	2.3	4.4	3.7
Tb	1.51	0.99	0.96	0.87	0.96	0.64	1.04	0.85	0.32	0.66	0.58
Dy	8.6	5.3	5.6	5.3	5.5	3.8	6.6	5.3	1.99	3.5	3.1
Ho	1.72	1.08	1.10	0.98	1.07	0.77	1.39	1.18	0.40	0.70	0.64
Er	5.0	3.0	3.1	2.7	3.2	2.2	4.0	3.3	1.22	2.0	1.85
Tm	0.73	0.43	0.47	0.39	0.49	0.36	0.66	0.53	0.20	0.30	0.29
Yb	4.5	2.9	3.1	2.5	3.3	2.3	4.3	3.4	1.44	2.00	2.1
Lu	0.67	0.42	0.45	0.39	0.53	0.35	0.64	0.52	0.23	0.32	0.32
Hf	7.3	6.1	6.6	6.5	18.5	16.9	9.4	7.5	3.9	5.2	5.5
Ta	1.10	1.25	1.55	1.24	1.46	1.03	3.3	2.8	2.0	2.1	2.1
Th	2.5	3.9	8.0	6.0	5.8	1.99	16.7	19.1	31	22	25
U	0.91	1.88	2.1	1.20	2.9	1.04	2.8	2.8	5.6	1.83	1.54

Table 1. (Contd.)

Components	Moderately alkaline leucogranites						Fe-eckermannite leucogranites				
	X-1543	X-1547	X-1548	X-1560	K17-7	K17-8	K19-24	K19-27	K19-28	K19-29	K19-31
SiO_2	76.11	76.97	76.05	75.15	77.03	76.80	75.42	74.88	73.10	75.01	74.55
TiO_2	0.22	0.12	0.23	0.16	0.16	0.16	0.08	0.07	0.06	0.09	0.07
Al_2O_3	12.45	12.24	12.41	12.70	12.04	12.19	11.63	11.73	13.23	12.18	12.64
$Fe_2O_3^*$	1.33	0.93	1.33	1.56	1.36	1.16	2.91	3.18	2.67	2.85	2.80
MnO	0.01	0.02	0.03	0.04	0.04	0.03	0.06	0.07	0.06	0.05	0.06
MgO	0.15	0.05	0.15	0.11	0.09	0.10	0.05	0.03	0.03	0.07	0.05
CaO	0.28	0.38	0.36	0.41	0.38	0.47	0.13	0.08	0.05	0.08	0.18
Na_2O	3.21	3.71	3.59	3.89	3.66	3.67	4.46	4.53	5.07	4.55	5.38
K_2O	5.34	4.55	4.95	5.03	4.77	4.83	4.13	4.63	4.70	4.17	3.54
P_2O_5	0.03	0.01	0.03	0.03	0.02	0.02	0.01	0.01	0.01	0.01	0.02
L.O.I.	0.49	0.11	0.23	0.37	0.21	0.29	0.45	0.39	0.31	0.55	0.32
Total	99.70	99.14	99.45	99.54	99.82	99.80	99.38	99.67	99.32	99.67	99.68
Rb	117	75	158		207	224		401		389	362
Sr	63	7.9	30		11.7	10.4		7.2		6.1	8.3
Y	23	6.0	20		20	24		107		270	108
Zr	173	125	197		169	161		113		1330	292
Nb	44	8.6	31		38	54		19.3		158	51
Cs	1.67	0.27	1.70		3.9	4.9		5.5		4.1	3.0
Ba	261	43	206		49	45		34		14.3	16.0
La	63	21	33		42	48		56		165	55
Ce	82	35	62		72	81		145		354	136
Pr	9.0	3.4	7.1		7.0	8.2		21		70	16.1
Nd	28	11.3	24		21	25		73		278	58
Sm	4.5	1.88	4.1		3.5	3.9		21		90	17.0
Eu	0.51	0.16	0.45		0.23	0.23		0.30		1.15	0.26
Gd	4.3	1.32	3.7		3.1	3.4		22		91	16.9
Tb	0.66	0.19	0.61		0.48	0.53		3.4		14.0	3.0
Dy	3.6	1.05	3.7		3.0	3.3		18.0		75	19.2
Ho	0.72	0.22	0.73		0.63	0.71		2.8		12.3	3.6
Er	2.1	0.74	2.2		2.0	2.3		6.1		28	10.0
Tm	0.35	0.14	0.35		0.34	0.37		0.80		3.3	1.41
Yb	2.4	1.08	2.4		2.6	2.8		5.5		20	9.3
Lu	0.35	0.19	0.35		0.41	0.45		0.95		2.9	1.41
Hf	6.2	4.6	6.0		6.2	6.3		6.3		41	11.6
Ta	3.3	0.36	2.9		3.3	5.8		0.89		11.0	3.0
Th	37	22	25		36	39		4.4		50	14.4
U	2.2	2.4	4.1		4.2	8.8		0.91		11.6	3.4

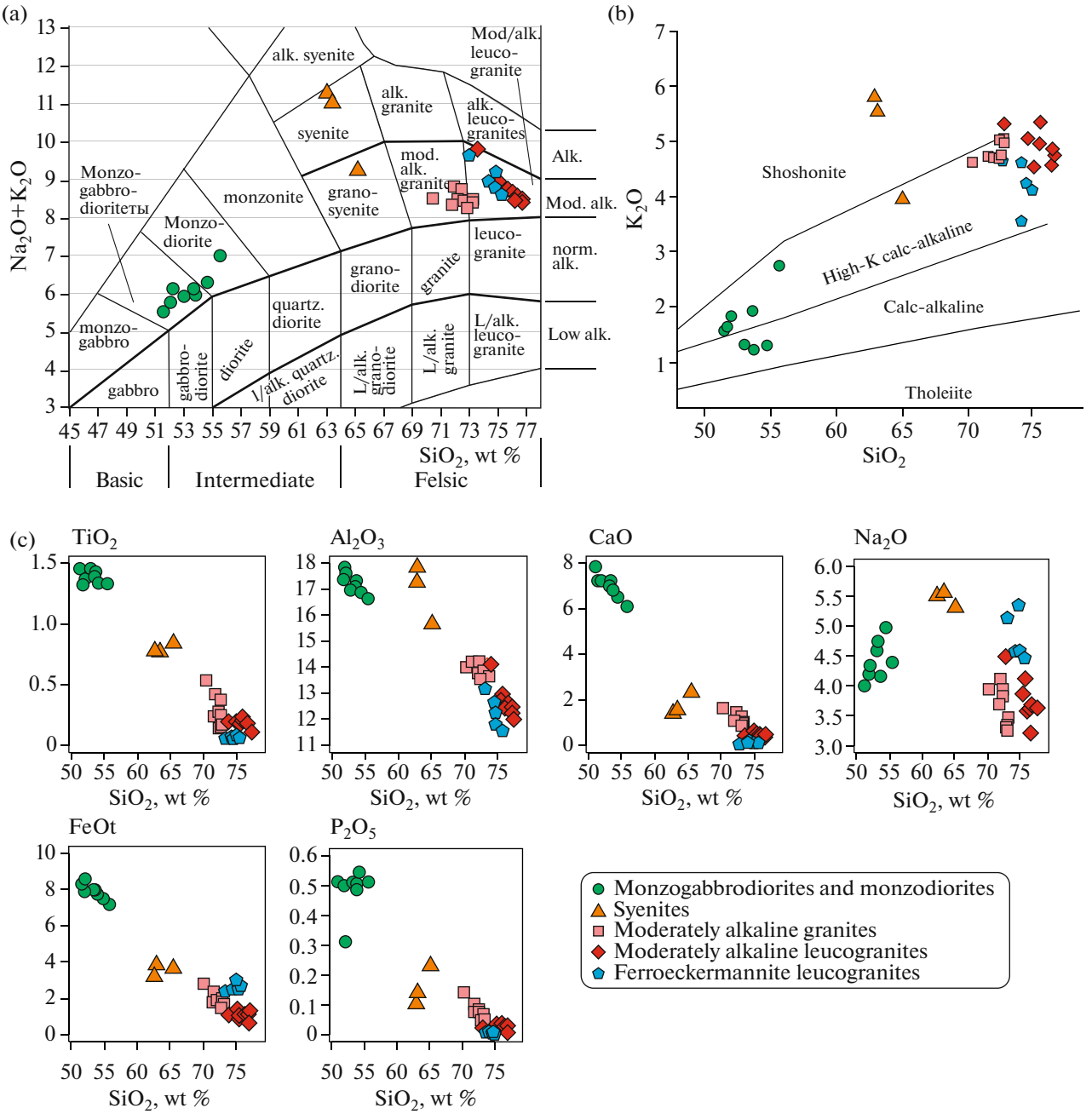

Fig. 5. Composition of major components of the Akzhailau massif in the TAS-diagram (Sharpenok et al., 2013) (a), in the diagram SiO_2–K_2O (Rickwood, 1989) (b), and in the binary diagrams (c). Contents of all oxides are given in wt %.

La_n/Yb_n = 8.2–8.83, total REE is 144.08–241.33 ppm. The multielement patterns show negative P and Ti anomalies, and a positive Zr anomaly. Sample X-1561 has the high Ba = 3591 ppm (in other syenite samples Ba = 982–1864 ppm).

Moderately alkaline granites contain (in wt %): SiO_2 70.5–73.8, CaO 0.91–1.54, Al_2O_3 13.7–14.35, TiO_2 0.17–0.54, (Na_2O + K_2O) = 8.35–8.82 with K_2O/Na_2O = 1.15–1.55; femic components (FeO + Fe_2O_3 + MgO) = 1.76–3.85 wt % with FeO*/(FeO* + MgO) = 0.82–0.87; high Ba 549–1050 ppm. In the TAS-diagram (Fig. 6), the composition points of given rocks are practically completely localized in the field of moderately alkaline granites and are ascribed to the high-K calc-alkaline series according to the SiO_2–K_2O diagram. The REE pattern shows the LREE predominance over HREE, a negative Eu-anomaly (Eu/Eu*) = 0.83–0.88, La_n/Yb_n=8.2–8.8, and total REE = 113–228 ppm. The multielement patterns display negative Ba, Nb, P, and Ti anomalies and positive Th and Zr anomalies.

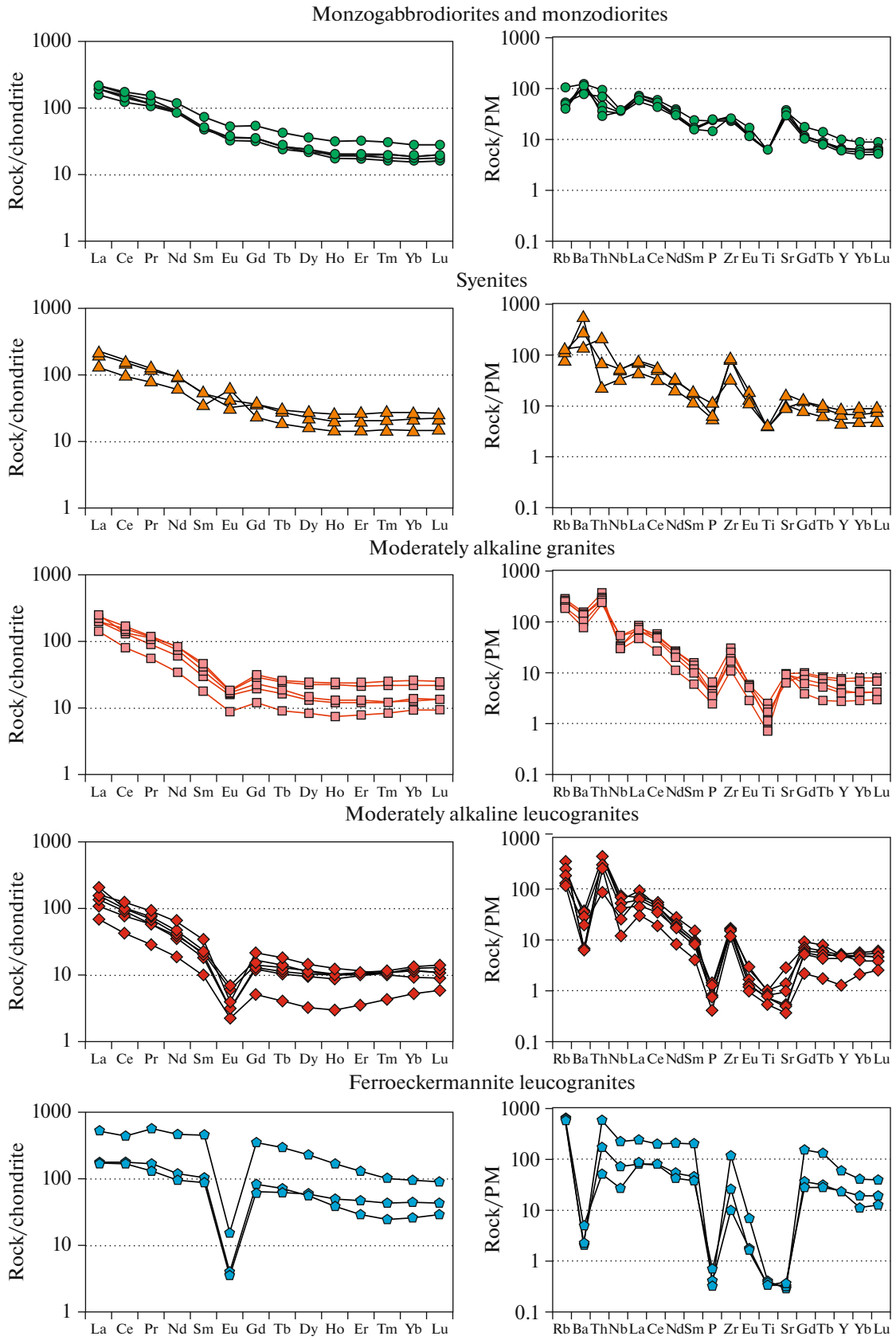

Fig. 6. C1-normalized (Boynton, 1984) rare-earth element distribution patterns (in the left side) and primitive mantle (PM)-normalized (Sun and McDonough, 1989) pattern (in the right side).

Moderately alkaline leucogranites contain (in wt %): SiO_2 73.5–77.6, CaO 0.28–0.47, Al_2O_3 12.05–14.25, TiO_2 0.12–0.23, (Na_2O + K_2O) = 8.33–9.8 with K_2O/Na_2O = 1.1–1.67; femic components (FeO + Fe_2O_3 + MgO) = 0.99–1.67 wt % with FeO*/(FeO* + MgO) = 0.89–0.94. In the TAS-diagram (Fig. 6), data points of the given rocks are localized in the field of moderately alkaline leucogranites and are ascribed to the high-K calc-alkaline series according to the SiO_2–K_2O diagram. The REE pattern demonstrates LREE predominance over HREE, a negative Eu-anomaly (Eu/Eu*) = 0.14–0.35, La_n/Yb_n = 9.33–17.71, and total REE 77–222 ppm. Multielement patterns show negative Ba, P, Nb, Ti, and Sr anomalies and positive Th and Zr anomalies.

Ferroeckermannite leucogranites contain (in wt %): SiO_2 73.6–75.9, CaO 0.05–0.18, Al_2O_3 11.7–13.32, TiO_2 0.05–0.09, (Na_2O + K_2O) = 8.65–9.83 with K_2O/Na_2O = 0.66–1.03; femic components (FeO + Fe_2O_3 + MgO) = 2.71–3.22 wt % with FeO*/(FeO* + MgO) = 0.97–0.99. In the TAS-diagram (Fig. 6), data points of the rocks are localized in the field of moderately alkaline leucogranites and belong to the high-K calc-alkaline series in the SiO_2–K_2O diagram. The REE patterns display a pronounced negative Eu anomaly (Eu/Eu*) = 0.04–0.05, LREE predominance over HREE, La_n/Yb_n = 3.96–6.87, total REE 347–1204 ppm. Multielement patterns reveal negative Ba, P, Nb, Ti, and Sr anomalies and positive Zr and Th anomalies.

Geochronological Data

The age of the Akzhailau massif was determined by U-Pb LA-ICP-MS zircon dating and Ar-Ar amphibole dating.

The monzogabbrodiorites and monzodiorites contain thin strongly elongated grains of prismatic zircon from 200 to 300 μm; cathodoluminescence images of zircons from monzodiorites show no zoning; scarce grains have a weakly expressed zoning as well as distorted zoning (Fig. 7). Obtained age on 39 experimental points equals 294 ± 2 Ma (sample X-1556).

For Ar-Ar isotope dating, amphibole monofraction corresponding to magnesian hornblende (aliquot of 80–100 mg) was extracted from monzodiorite sample (sample X-1556). The unaltered largest grains 300–500 μm in size were hand-picked under binocular microscope. The $^{40}Ar/^{39}Ar$ spectrum (sample X-1556) shows a steady plateau corresponding to 75% released ^{39}Ar, which corresponds to the age of 289 ± 7 Ma (Fig. 8). This age within error corresponds to that established by U-Pb method on zircon.

Syenites (sample X-1561) contain large (200–300 μm) prismatic zircon with well-shaped bipyramids. Zircons from syenites are peculiar in the presence of cores: central parts of the grains in cathodoluminescence are represented by darker domains with weakly expressed zoning or without it, and frequently rounded shape. The cores are fringed by light rim with oscillatory zoning. There are also some granites with oscillatory zoning without cores. U-Pb dating was carried out both for domains with oscillatory zoning and for cores. The age obtained on the core-free zircons and rims is 295 ± 1 Ma on 19 points; the cores have slightly older age of 301 ± 1 Ma.

Moderately alkaline granites contain zircons 150–250 μm in size, with short-prismatic habit and developed bipyramid (sample K19-34). In the cathodoluminescence images, zircons have expressed oscillatory zoning, some grains have darker cores, as well as contain numerous inclusions; scarce domains have disturbed zoning. Obtained age equals 292 ± 3 Ma (based on 16 points), two dated zircon cores yielded an age of 386–387 Ma, which corresponds to the Middle Devonian.

Moderately alkaline leucogranites contain large zircons ~ 300–400 μm with bipyramidal prismatic habit. In the cathodoluminescence images, zircons have dark shells with well-expressed oscillatory zoning. These zircons contain numerous mineral inclusions, which are seen in a transmitted light, which frequently results in incorrect values during laser ablation dating. Moderately alkaline leucogranites give an age of 301 ± 1 Ma (sample X-1548, 25 points), and 308 ± 6 Ma (sample K17-6, 10 points).

Ferroeckermannite leucogranites. Three U-Pb dates were obtained by different methods for rocks of this group: 292 ± 2 Ma (albitized granite, SHRIMP-II, CIR VSEGEI, Frolova, 2018), 287 ± 4 Ma (apogranite, LA-ICP-MS, Museum of Natural History, London, Baisalova, 2018), and 283 ± 4 Ma (granite, SHRIMP-II, CIR VSEGEI, Levashova et al., 2022). Geochronological studies were performed for the zircon monofraction separated from sample K19-25 of ferroeckermannite leucogranite. The zircons have small sizes (100–200 mm), unclear morphology, frequently with uneven dissolved rims. In the cathodoluminescence images, the zircons contain numerous light inclusions and metamict inner structure. Obtained U-Pb age is 290 ± 3 Ma (10 points). In addition, we dated ferroeckermannite monofraction. The $^{40}Ar/Ar^{39}$ spectrum has plateau corresponding to 65% released ^{39}Ar. The plateau age is 281 ± 5 Ma (Fig. 8). Measured data coincide with previous dates of 292–281 Ma. Such a scatter could be related to the wide development of postmagmatic processes, which could lead to the metamictization of zircon grains, as well as high contents of rare-earth and radioactive elements in their inclusions (monazite, coffinite, plumbobetafite, and others).

Sm-Nd and Rb-Sr Isotope Composition

Results of determination of Rb-Sr and Sm-Nd isotope data are listed in Table 2 and Fig. 9. All obtained

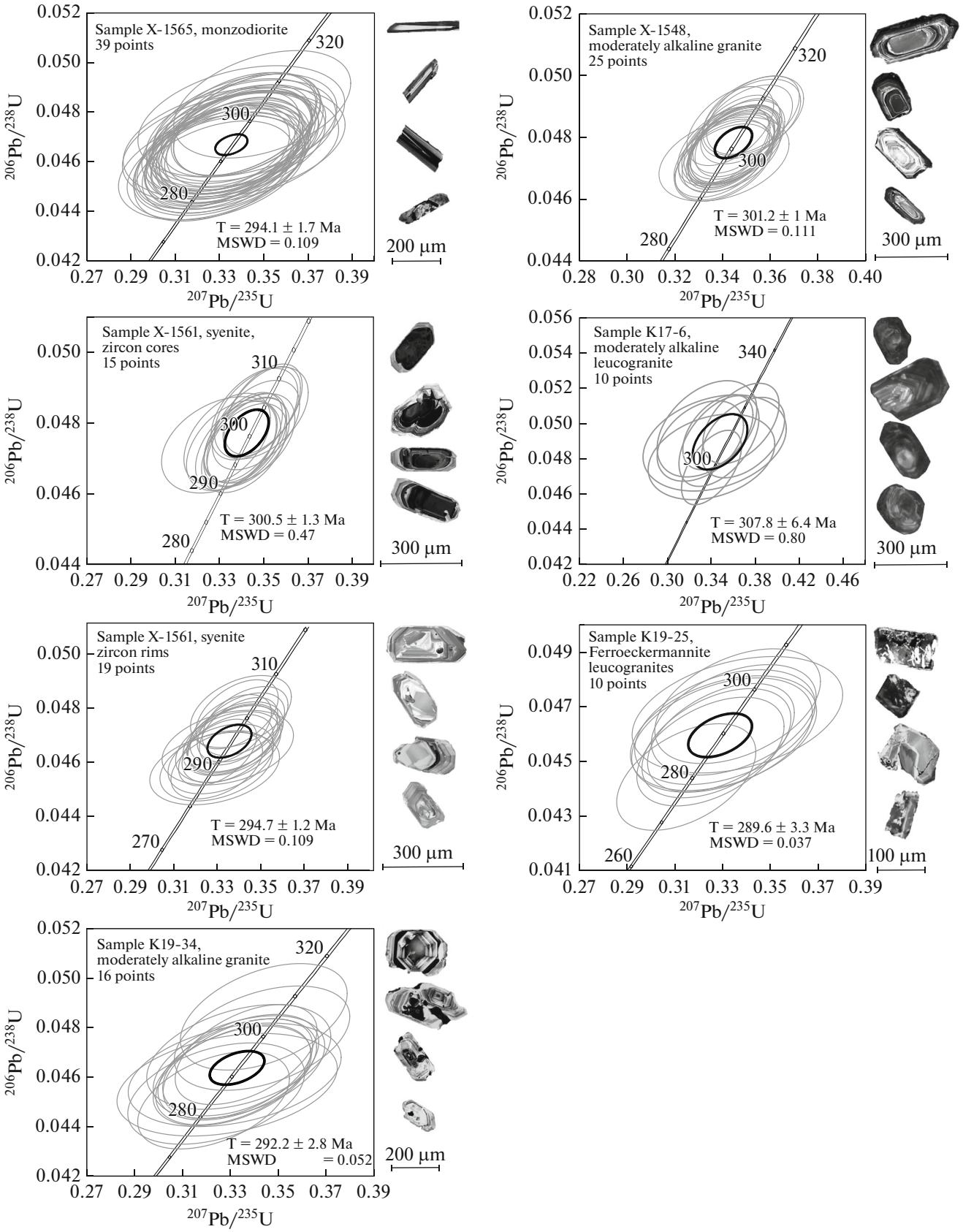

Fig. 7. Results of U-Pb isotope dating and cathodoluminescence images of representative grains from rocks of the Akzshailu massif.

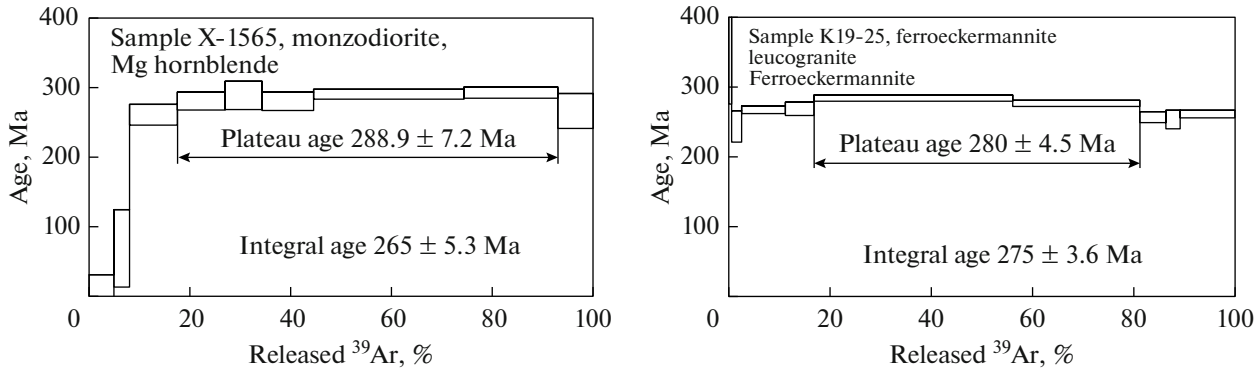

Fig. 8. Results of Ar-Ar isotope dating of amphiboles from rocks of the Akzhailau massif.

ε_{Nd} values on the rocks of the Akzhailau massif are sufficiently close and show a relatively low maturity of possible protoliths of the granitoids. The monzogabbrodiorites (samples X-1554 and X-1556) are characterized by the highest $\varepsilon_{Nd}(T)$ = +4.57 and +5.82 ($T_{Nd}(DM\text{-}2st)$ = 658 and 559 Ma) among massif. Syenites (sample X-1545), moderately alkaline granites (sample X-1550), and moderately alkaline leucogranites (sample X-1547) are characterized by the practically identical values of $\varepsilon_{Nd}(T)$ = +4.36...+4.50. The model ages of these rocks vary within $T_{Nd}(DM\text{-}2st)$ = 664–674 Ma. The isotope compositions of ferroeckermannite leucogranites are close to those obtained for monzogabbrodiorites $\varepsilon_{Nd}(T)$ = +5.64 ($T_{Nd}(DM\text{-}2st)$ = 574 Ma).

The Rb/Sr isotope ratios obtained for the rocks of the Akzhailau massif vary within sufficiently wide ranges. Thereby, values obtained for the monzodiorites and syenites are close: $(^{87}Sr/^{86}Sr)_T$ = 0.70382 and 0.70376, respectively. Values obtained for the studied granitoids have significant differences: they are much higher in moderately alkaline granites compared to the moderately alkaline leucogranites (0.70530 and 0.70062, respectively). The ferroeckermannite granites have $(^{87}Sr/^{86}Sr)_T$ = 0.647402. Such low $(^{87}Sr/^{86}Sr)_T$ values for the moderately alkaline ferroeckermannite leucogranites are incorrect due to the low Sr content in these rocks and should be ignored.

DISCUSSION

Classification and Geochemical Types of the Rocks

The granitoid rocks of the Akzhailau massif were classified using petrochemical classification based on three indicator indices: Fe mole fraction (FeO*/(FeO* + MgO)), MALI ($Na_2O + K_2O - CaO$), and ASI ($Al/(Ca - 1.67P + Na + K)$) (Frost et al., 2001) (Figs. 10a–10c). Compositions of all granitoids of the Akzhailau massif fall in the field of Fe-rich rocks, but ferroeckermannite (FeO*/(FeO* + MgO) = 0.97–0.99) and moderately alkaline leucogranites (FeO*/(FeO* + MgO) = 0.89–0.94) have higher Fe indices compared to the moderately alkaline granites (FeO*/(FeO* + MgO) = 0.82–0.87) and syenites (FeO*/(FeO* + MgO) = 0.79–0.89). Based on the MALI index, the main vol-

Table 2. Nd and Sr isotope composition in the rocks of the Akzhailau massif

Sample no.	Rock	Age	Sm	Nd	$^{147}Sm/^{144}Nd$	$^{143}Nd/^{144}Nd$	$\varepsilon_{Nd}(T)$	$T_{Nd}(DM\text{-}2st)$	Rb	Sr	$^{87}Rb/^{86}Sr$	$^{87}Sr/^{86}Sr$	$(^{87}Sr/^{86}Sr)_T$
X-1556	Monzodiorite	294	7.7	42	0.1088	0.51277	+5.82	559	66	663	0.28744	0.70502	0.703817
X-1564	Monzodiorite	294	7.4	38.3	0.1167	0.51272	+4.57	658	–	–	–	–	–
X-1545	Syenite	295	8.1	43.5	0.1162	0.51271	+4.50	664	52	212	0.69585	0.70668	0.703759
X-1550	Ultra-alkaline granite	292	7.3	40.0	0.1106	0.51269	+4.41	671	177	210	2.3137	0.71491	0.705298
X-1547	Ultra-alkaline leucogranite	301	1.8	11.1	0.1006	0.51268	+4.36	674	158	30	16.51553	0.77136	0.700620
K19-27	Fe-eckermannite leucogranite	290	23	85	0.1629	0.51286	+5.64	574	389	6.1	224.730	1.57475	0.647402

* Age and model age ($T_{Nd}(DM\text{-}2st)$) of the rocks are given in Ma; element concentrations are given in ppm.

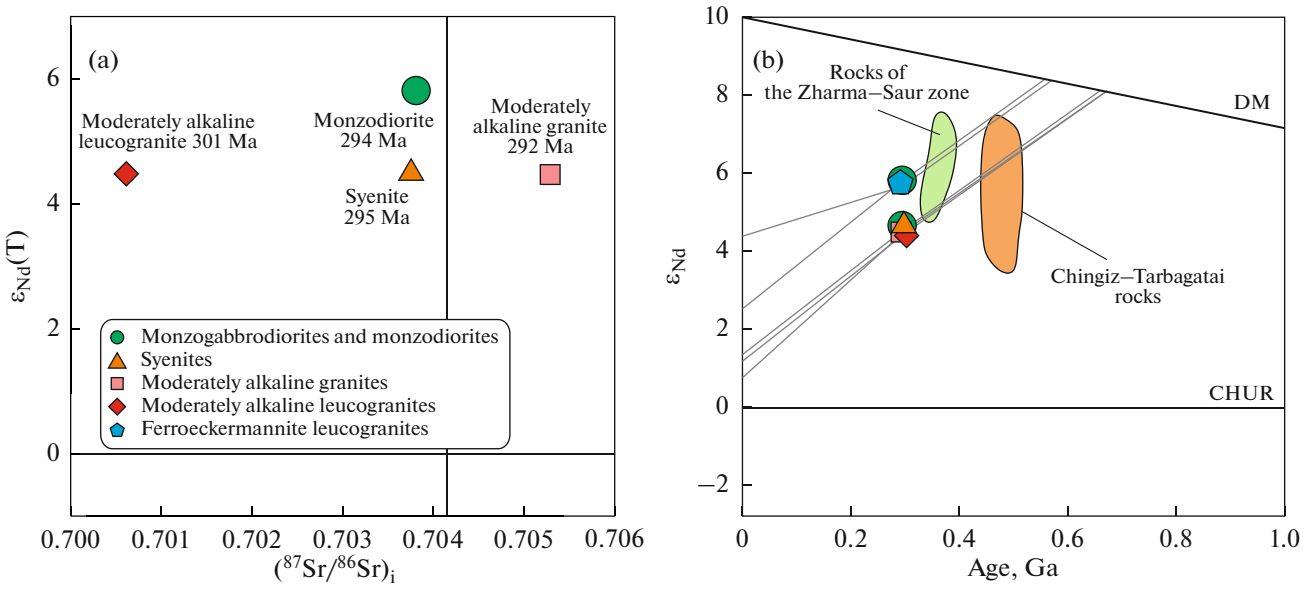

Fig. 9. Results of determination of Sm-Nd and Rb-Sr isotope compositions of rocks of the Akzhailau massif in the diagrams $(^{87}Sr/^{86}Sr)_i$–$\varepsilon_{Nd}(T)$ (a) and ε_{Nd}–age (b).

ume of rocks of the Akzhailau massif is ascribed to the calc-alkaline type. All studied syenites, as well as some ferroeckermannite and moderately alkaline leucogranites fall in the field of alkaline rocks. In the diagram ASI–A/NK, the compositions of moderately alkaline granites and leucogranites fall in the field of weakly peraluminous rocks ($1 < ASI < 1.1$). Syenites and monzodiorites are ascribed to the moderately-aluminum varieties, while ferroeckermannite granites belong to the alkaline varieties ($(Na + K) > Al$).

Further classification of the rocks of the Akzhailau massif (besides monzogabbrodiorites) was performed using "alphabetic" nomenclature proposed and developed in the works (Chappell and White, 1974; Collins et al., 1982; Barbarin, 1999; Eby, 1992). The petrogenesis of these rocks and potential sources are considered below.

Monzogabbrodiorites and monzodiorites are characterized by the lowered silica content, elevated contents of mafic components (Fig. 5), weakly expressed Eu- and Nb-minima, and high isotope values $\varepsilon_{Nd}(T) = +4.57$ and $+5.82$. They likely were derived from parental mantle-derived basite magmas. Judging from the high concentrations of LREE, Rb, Ba, and K_2O, parental basite magmas were subalkaline and high-potassium. Based on the geochemical characteristics, they could be correlated to the within-plate or ocean-island basalts (Fig. 10d). Similar geochemical characteristics are typical of the Early Permian ultrabasite–basite rocks forming minor intrusions of the Agrimbai and Maksut complexes, which compose the multiphase gabbro–monzodiorite–granite plutons in the conjugate Char zone of Eastern Kazakhstan (Khromykh et al., 2019). The possible source of basite magmas could be lithospheric mantle underlying the orogenic buildup (Khromykh, 2022).

Syenites. According to the classification (Frost et al., 2001), these are alkaline, high-Fe, low-Al rocks. They contain Ba-feldspar, Fe-rich biotite, and Fe-rich amphibole (ferroedenite). Accessory minerals in syenites contain titanite, Ce-bearing apatite, ilmenite, magnetite, monazite, and epidote. They are also characterized by the high Ba contents (982–3591 ppm). According to these data, syenites can be classified as I-type high-K granites (Barbarin, 1999).

Moderately-alkaline granites. Based on the petrogeochemical characteristics, they are intermediate between magnesian and ferroan series, weakly peraluminous, and calc-alkaline rocks (Figs. 10a–10c). Data points of their compositions in the diagram (Pearce et al., 1984) plot in the boundary of fields of volcanic-arc, syncollisional, and within-plate granites (Fig. 10e). Based on the presented data, the moderately alkaline granites can be considered as I-type granites or transitional granites between I- and S-types. Thereby, trends of decreasing P_2O_5 content and some trace elements with increasing SiO_2 argue in support of I-type granitoids.

Moderately-alkaline leucogranites. According to the petrochemical classification (Frost et al., 2001), these rocks correspond to the alkaline–alkali-calc series, are ferroan and weakly peraluminous (Figs. 10a–10c). Based on the major element relations in the diagram (Grebennikov, 2014), they correspond to A_2-type granitoids (Fig. 10f). At the same time, the high-field strength element contents (Zr, Nb, Ce, Y) in these rocks are similar to those of moderately alkaline gran-

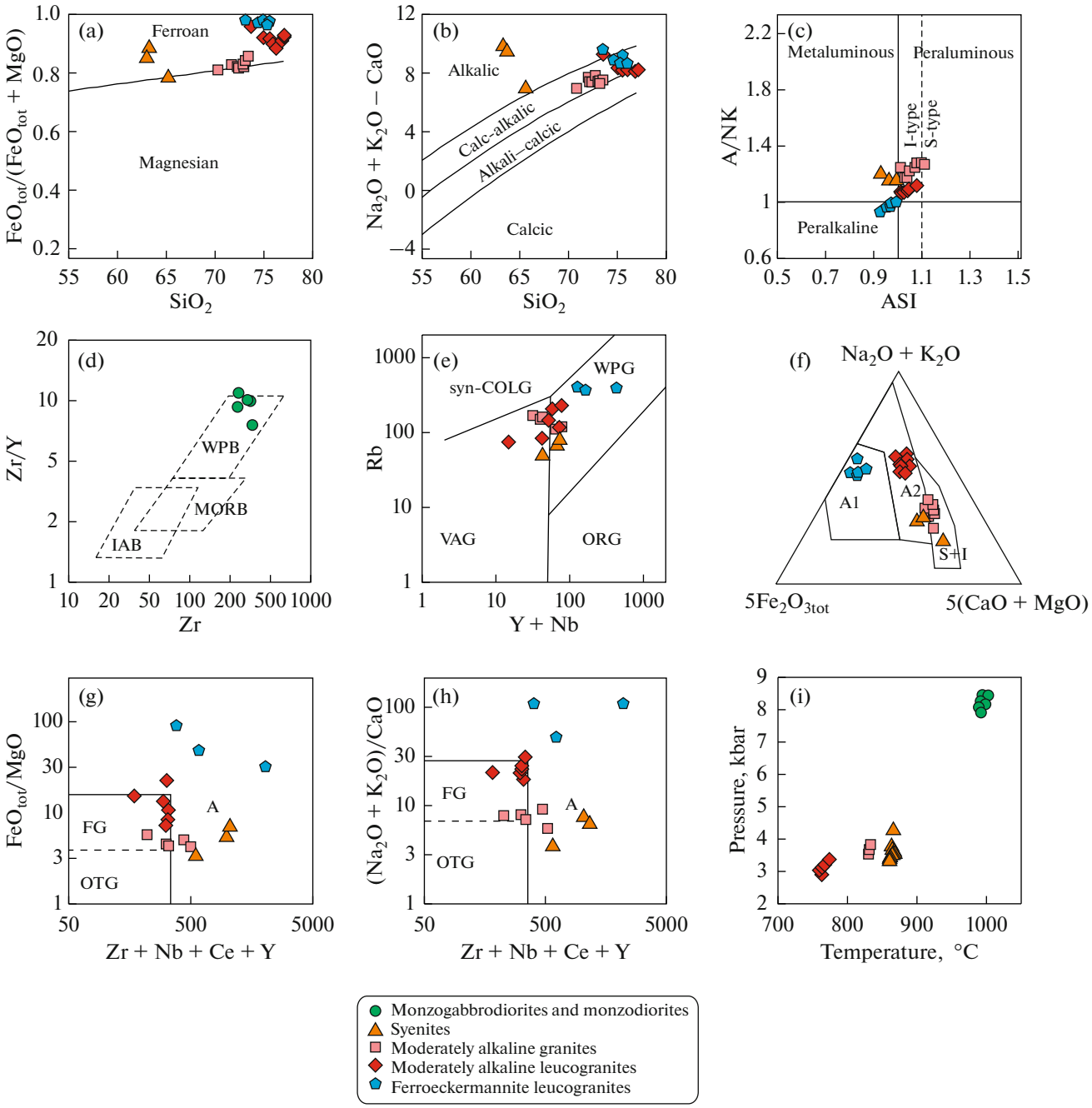

Fig. 10. Geochemical classification of granitoids of the Akzhailau massif in the diagrams. (a) SiO_2–$FeO_{tot}/(FeO_{tot} + MgO)$ (Frost et al., 2001); (b) SiO_2–MALI (Frost et al., 2001); (c) $Al_2O_3/(CaO + Na_2O + K_2O)$–ASI, mol % (Frost et al., 2001); (d) Zr–Zr/Y (Pearce and Norry, 1979) fields: (IAB) island-arc basalts, (MORB) mid-ocen ridge basalts, (WPB) within-plate basalts; (e) Rb–(Y + Nb) (Pearce et al., 1984) fields: (VAG) volcanic arc granites, (syn-COLG) syncollisional granites, (WPG) within-plate granites; (ORG) ocean-ridge granites; (f) $(Na_2O + K_2O)$–$Fe_2O_{3tot} \times 5$– $(CaO + MgO) \times 5$, mol %. (Grebennikov, 2014); (g) Zr + Nb + Ce + Y vs. FeO_{tot}/MgO (Whalen et al., 1987) fields: (FG) fractionated granites, (OFG) non-fractionated granites; (h) Zr + Nb + Ce + Y vs. $(Na_2O + K_2O)/CaO$ (Whalen et al., 1987); (i) and results of determination of *P-T* parameters of the formation of rocks of the Akzhailau massif.

ites in the diagrams (Whalen et al., 1987) and are plotted on the boundary between fractionated and A-type granites (Figs. 10g, 10h).

Ferroeckermannite leucogranites are made up of K-feldspar predominating over albite, alkaline amphibole (ferroeckermannite), and aegirine. Accessories are zircon, LREE fluorides and oxides, Nb-bearing hematite, as well as Th and As oxides. The leucogranites are alkalic to alkali–calcic according to the MALI index, peralkaline in terms of ASI index, and

extremely high-F rocks. As moderately alkaline leucogranites, these rocks have the high Rb/Sr ratio, low CaO, extremely high contents of high-field strength elements (Nb, Ta, Zr, Y), and low Sr, P, and Ti contents. Ferroeckermannite leucogranites could be unambiguously ascribed to the A-type granites (Figs. 10f, 10g, and 10h), more precisely, to the A_1-type granites based on the content of indicator elements.

Petrogenesis

The wide development of I-type granites within the Akzhailau massif (>70%) suggests that the magma formation was mainly controlled by partial melting of crustal protoliths. The moderate aluminum content of magmas suggests the absence of mature sedimentary complexes (aluminous shales, siltstones, and others) and the predominance of volcanic and volcanogenic-sedimentary rocks in the potential sources. The wide development of relatively low-Si I-type syenites indicates that they were derived through sufficiently high melting degree from a relatively low SiO_2 protolith, i.e., from mafic and intermediate rocks.

Close trace-element concentrations of moderately alkaline leucogranites and moderately alkaline granites, as well as similar Nd isotope characteristics suggest a genetic affinity of the leucogranites classified as A_2-type and I-type granites. The leucogranites compared to the granites demonstrate strong depletion in Sr, Ba, Eu, and P, which can be caused by the fractionation of plagioclase and K-feldspar. The fractionation of feldspars during crystallization of granitoid magmas is unusual due to the high viscosity of melts, thus indicating that compositional difference was presumably provided by partial melting. We may suggest that A_2-leucogranites and granites were formed by melting of crustal protoliths of similar composition at different degree of melting.

At present, several different models are proposed to explain the formation of A_1-type granites similar to the ferroeckermannite leucogranites of the Akzhailau massif. Among these models are both differentiation of alkaline mantle-derived magmas (Eby, 1990) and melting of different lower crustal protoliths (Whalen et al., 1987) or protoliths of the higher crustal levels (Patiño Douce, 1999; Tsygankov et al., 2021).

For the Akzhailau massif, the presence of subsimultaneous highly alkaline basite magmas, close Nd isotope characteristics, and small volumes of alkaline granites suggest the formation of ferroeckermannite leucogranites through the differentiation of alkaline basite magmas. The differentiation likely occurred at relatively great depths, which exceeded the generation level of other granitoids of the massif: in the lower–middle crust. However, the high SiO_2 content (>73 wt %) cast some doubts concerning the formation of leucogranites by differentiation of basite magmas due to the significant number of intermediate chambers and increase of magma viscosity. At the given stage, available data are insufficient to propose a definite model of formation of ferroeckermannite magmas. It is quite possible that these rocks were formed through combined differentiation and contamination.

Potential Sources of Granitoids

Within the western part of the Zharma–Saur zone, the modern erosion surface is practically completely represented by sedimentary rocks of the Kokon Formation. According to (Degtyarev, 2012), the base of this test site likely consists of the Early Paleozoic rocks--fragments of Caledonian island arcs, which were accreted to form the Kazakhstan composite continent (Chingiz–Tarbagatai zone). The possible basement of the western part of the Zharma–Saur zone could be the Devonian–Early Carboniferous volcanosedimentary complexes of the Zharma–Saur island arc. The Zharma–Saur island arc is composed of the basalts, basaltic andesites, and andesites, while sedimentary rocks in the western part, including the rocks of the Kokon Formation, represent the disintegration products of this arc and Caledonian Chingiz arcs. The comparison of isotope characteristics of potential sources and rocks of the Akzhailau massif is shown in Fig. 9. The isotope composition of the considered granitoids corresponds to the field of volcanics developed within the Chingiz–Tarbagatai zone (Degtyarev et al., 2015) and the rocks of the Zharma–Saur island arc (author's unpublished data). In other words, available data are insufficient to determine which complexes compose the base of the western part of the Zharma-Saur zone and which complexes are sources of the considered granitoids: Early Paleozoic or Middle–Late Paleozoic. Anyways, this source was volcanic or volcanosedimentary island-arc rocks (basalts, basaltic andesites, and others), which is correlated to the wide development of syenites and I-type granites in the Akzhailau massif.

P-T Parameters of the Magma Generation

The *P-T* parameters of the granitoid formation were determined using biotite–melt geobarometer constructed by machine learning method based on experiments on melting of different protoliths (Li and Zhang, 2023). This thermobarometer spans a significant range of temperatures and pressures (T = 625–1325°C, P = 1–48 kbar), as well as makes it possible to estimate the generation parameters of all granitoid phases of the Akzhailau massif (besides ferroeckermannite leucogranites), because biotite is an ubiquitous mineral. Results of the analysis are presented in Fig. 10i. According to obtained data, the lowest temperatures within 755–765°C were obtained for the moderately alkaline leucogranites. These rocks also gave the lowest pressure estimates of 2.8–3 kbar. The moderately alkaline granites yielded the higher tem-

peratures 800–835°C and pressure variations from 3.9 to 4.8 kbar. In spite of the total deficiency in analyses of biotites from moderately alkaline granites, estimates obtained on them correspond to *P-T* parameters determined on similar granites from conjugate massifs of the Zharma–Saur zone (author's unpublished data). Syenites from the Akzhailau massif according to estimates of this geothermobarometer define the formation temperature 855–876°C and pressure from 3.4 to 4.9 kbar. The highest temperature and deepest-seated magmas are monzogabbrodiorites, which are characterized by temperature reaching 1000°C (988–1002°C) and pressure above 8 kbar (8.1–8.5 kbar).

The comparison of obtained data show that the main volume of syenites and granites was formed at sufficiently close estimates of 3–4 kbar, which corresponds to depths of 9–12 km. To a first approximation, this agrees with geophysical data (Ermolov et al., 1977) indicating that the root system of the intrusion is traced to depths of ~13 km. An increase of melting temperature from the highest silica leucogranites to granites and syenites suggests that compositional variations of melts, first of all, were determined by the degree of protolith melting. Thus, low melting degree at low temperatures resulted in the formation of leucogranites, while increasing temperature led to the increase of melting degree and formation of syenites.

Petrological Model and Geodynamic Interpretation

Judging from isotope data, syenites, moderately alkaline granites, and leucogranites were formed through melting of compositionally close protolith, which also indicates a "petrological homogeneity" of rocks of the studied block at depths of 10–15 km. An increase of obtained temperature estimates is consistent with decreasing silica content in the rocks of the Akzhailau massif: syenites (63–65 wt % SiO_2) – 855–876°C, granites (70–73 wt % SiO_2) – 800–835°C, and leucogranites (75–77 wt % SiO_2) – 755–765°C. This dependence, similar isotope composition, and close pressure estimates allow us to propose that the syenite–granite–leucogranites were derived through melting of the same protolith at different melting degree. Based on U-Pb isotope dating, the formation of the lowest temperature moderately alkaline leucogranite melts predated the formation of high-temperature varieties. Since the age estimates of the formation of syenites and moderately alkaline granites are almost identical, the sequence of generation of these two phases cannot be established. Based on the geological structure of the massif where moderately alkaline granites partially occupy an axial position, the moderately alkaline granites could be produced by fractionation of initial syenite magmas.

The generalization of geological (Fig. 1), geochronological (Figs. 7, 8, 11), petrogeochemical, and isotope (Figs. 5, 6, 9, 10) data allowed us to formulate a general model of the formation of the Akzhailau pluton. The first stage (308–300 Ma) produced moderately alkaline leucogranites. The second stage within 295–292 Ma is characterized by the emplacement of monzogabbrodiorites and monzodiorites and formation of syenites and moderately alkaline granites, which formed the main volume of the pluton. The third, final stage at ~289 Ma was responsible for the emplacement of dikes and stocks of alkaline (ferroeckermannite) leucogranites in the west and north of the pluton. Thus, the formation of the Akzhailau pluton spanned no more than 15 Ma, i.e., pluton was formed during a single endogenous event at the end of Carboniferous–beginning of the Early Permian. The presence of monzogabbrodiorites and monzodiorites as derivatives of basite magmas in the pluton testify that the formation of the plutons was triggered by underplating of parental basite magmas at the crustal base. This is also confirmed by the appearance of subsimultaneous basite magmatism in the adjacent Char zone of Eastern Kazakhstan: continental subalkaline basalts and andesites in the Saryzhal trough and Tyureshok basin at 297 ± 1 Ma (Khromykh et al., 2020), minor intrusions of subalkaline gabbro of the Argimbai complex at 293 ± 2 Ma (Khromykh et al., 2019).

Stage 1. The appearance of thermal source at the crustal base could cause an increase of temperature gradients, and, according to available concepts (Reverdatto et al., 2017), high-temperature metamorphism of the granulite facies. Thereby, a transition to the granulite facies metamorphism implies the dehydration of hydrous minerals (first of all, micas and amphiboles) and release of significant amount of fluids (Cuney and Barbey, 2014; Antipin et al., 2019). Fluids when reached the middle crustal levels, could cause migmatization and partial melting of protoliths with relatively low degree melting, thus likely producing small portions of leucogranite melts. This event occurred within 308–301 Ma and led to the formation of moderately alkaline leucogranites and their emplacement as the first intrusive phase of the massif.

Stage 2. Differentiation in the subcrustal basite chamber resulted in the formation of differentiated monzogabbroid and monzodiorite magmas. Based on the pressure estimates, the monzogabbrodiorite magmas were formed at depths near 25 km. Due to the lower density, according to the MASH model – Melting, Assimilation, Storage, and Homogenization (Sen, 2014), these magmas could reach the higher crustal levels. The influence of basite magmas on the previously heated crustal protoliths led to increasing scales and degree of partial melting of crustal protoliths, which resulted in the formation of less felsic syenite magmas and moderately alkaline granites, which occupy the most part of the Akzhailau pluton at the present-day erosion surface.

Stage 3. Last magmatic episode of the evolution of the Akzhailau massif was responsible for the intrusion

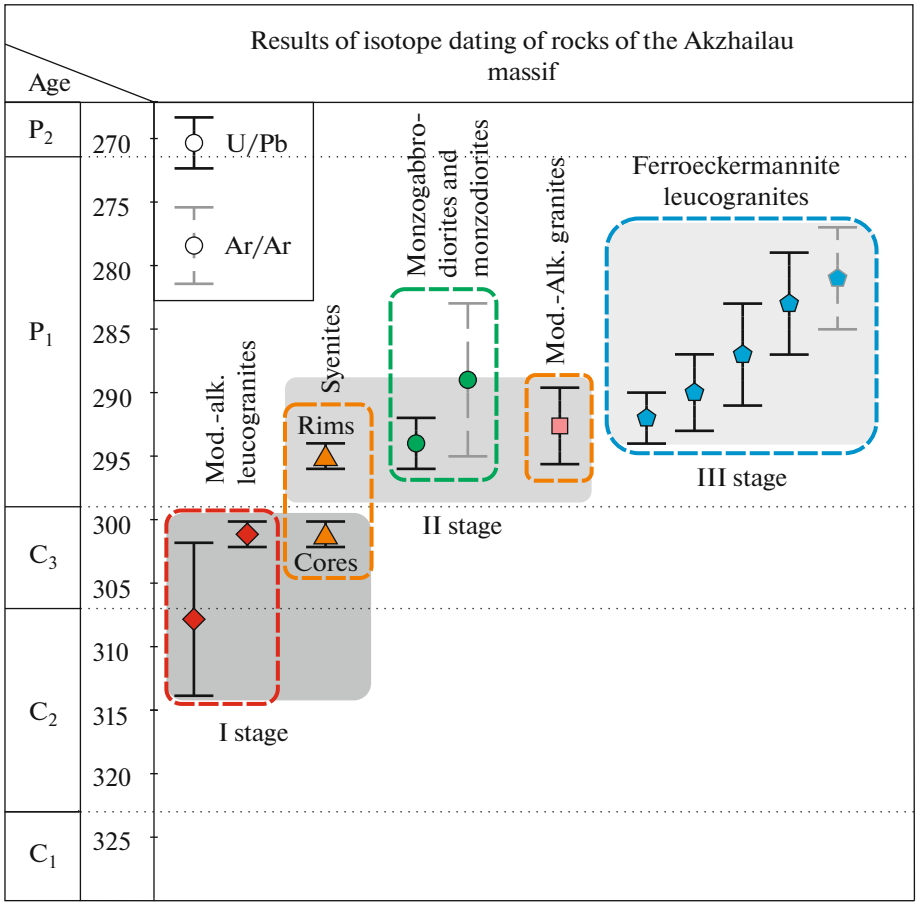

Fig. 11. Stages of the formation of the Akzhailau massif based on generalization of geochronological data. Authors data are supplemented by age data on the ferroeckermannite granites of the Bol'shoi Espe granite stock (Baisalova, 2018; Frolova et al., 2022; Levashova et al., 2022).

of dikes and minor bodies of the alkaline ferroeckermannite leucogranites, which could be derived through the differentiation of alkaline basite magmas or melting of lower crustal protoliths. The intrusion of alkaline leucogranite magmas in the higher crustal horizons became possible only after consolidation of the main volume of the massif and formation of fracture systems along which alkaline magmas penetrated as dikes.

The geodynamic settings of the magmatic rocks of the studied area are analyzed using data on the geological evolution of lithosphere of the region reported in (Shcherba et al., 1976; Ermolov et al., 1977, 1983; Khromykh, 2022). The formation of the orogenic fold system in the Zharma–Saur zone occurred in the end of Early Carboniferous–beginning of the Middle Carboniferous, which is marked by the accumulation of continental molasse with conglomerates at the base in the intermontane basins. At the early orogenic stages (Serpukhovian time), the Saur gabbro–diorite–granitoid series appeared within the Zharma–Saur zone. The granitoids in this series are represented by the Bugaz Complex (327–326 Ma) and are composed of the low-alkali biotite granodiorites with subduction-related geochemical affinity (Khromykh et al., 2019). The Middle Carboniferous was marked by the collapse of the orogenic buildup, which was accompanied by the strike-slip–pull apart movements along large regional faults and appearance of the continental basaltic andesite volcanism (311±3 Ma, Khromykh et al., 2020) and belts of the Middle Carboniferous basite dikes (315 ± 4 Ma, Khromykh et al., 2019).

The largest scale basite and granitoid magmatism spanned the entire Eastern Kazakhstan in the Early Permian; exactly this age (305–280 Ma) was determined for most granitoid massifs that formed the large Kalba and Zharma batholithic belts (Kotler et al., 2015; Khromykh et al., 2016, 2019; Kotler et al., 2021). The Early Permian basite magmatic complexes belong to the subalkaline series and have enriched geochemical characteristics, while granitoid plutons (and the Akzhailau pluton, first of all) are characterized by subsimultaneous formation of significant volumes of geochemically diverse granitoids with significant fraction of A-type rocks. The comparison of age and composition data on magmatism in the adjacent regions indi-

cates that the Tarim large igneous province caused by the Tarim mantle plume activity spanned the western CAOB, including the Southern and southwestern Mongolia, Tarim plate, Xingjian–Uigur region, Tien Shan, and Southern and Eastern Kazakhstan in the Early Permian (300–270 Ma) (Dobretsov et al., 2010; Yarmolyuk et al., 2014; Xu et al., 2014; Khromykh et al., 2019). In Eastern Kazakhstan, the influence of the Tarim mantle plume was expressed in increasing temperature gradients in the upper mantle and lithosphere, partial melting of mantle protoliths, and formation of subalkaline basite magmas, which ascended and interacted with metamorphic protoliths at the base of orogenic system formed during Carboniferous, thus causing large-scale crustal melting (Khromykh, 2022; Kotler et al., 2021; Khromykh et al., 2022). Precisely these processes were responsible for the formation of the Akzhailau granitoid pluton. Thus, the main geodynamic mechanisms of the formation of the studied pluton are the interaction of the plume-derived subalkaline basite magmas with metamorphosed crustal protoliths of orogenic system.

CONCLUSIONS

Based on the petrographic, chemical, geochronological, and isotope data, the Akzhailau massif was formed in three stages, which significantly differ from previously accepted concepts on the polychronous formation of this intrusion. The following stages are distinguished:

(1) Emplacement of A_2-type moderately alkaline leucogranites (308–300 Ma) owing to the dehydration of the lower crustal protoliths;

(2) Intrusion of monzogabbrodiorites (~295 Ma) in the leucogranites and formation of syenites and I-type moderately alkaline granites (294–292 Ma);

(3) Emplacement of dikes and minor bodies of A_1-type alkaline ferroeckermannite leucogranites (~289 Ma).

The granitoids of distinguished stages differ both in composition of rock-forming minerals and in major-, trace-element and isotope composition. The Akzhailau pluton was formed within ~15 Myr in the middle–upper crust at interaction of plume-related subalkaline basite magmas with metamorphosed crustal protoliths of orogenic system.

ACKNOWLEDGMENTS

We are grateful to O.N. Kuzmina for help with organization of field works in the Republic of Kazakhstan. N.G. Karmanova, I.V. Nikolaeva, and S.V. Palessky are thanked for the determination of rock composition, and N.G. Soloshenko, for the determination of Nd isotope composition.

FUNDING

Generalization and analysis of obtained materials were made in the framework of the government-financed program of the Institute of Geology and Mineralogy, Siberian Branch, Russian Academy of Sciences. Petrographic studies, analysis of major and trace elements were supported by the Russian Science Foundation (project no. 21-17-00175). U-Pb and Ar-Ar isotope dating was supported by the Russian Science Foundation (project no. 22-77-00061), analysis of Rb-Sr and Sm-Nd isotope composition was carried out in the framework of the grant from the President of the Russian Federation (MK-1870.2022.1.5).

CONFLICT OF INTEREST

The authors of this work declare that they have no conflicts of interest.

REFERENCES

Antipin, V.S., Perepelov, A.B., and Odgerel, D., Rare-metal granites from various zones of the Early Mesozoic magmatic areal (Mongolia): geochemical and petrogenetic features, *Dokl. Earth Sci.,* 2019, vol. 485, no. 3, pp. 317–321.

Baisalova, A.O., Metasomatic Processes of Rare-Metal Occurrences of the Akzhailautas Granite Massif and Adjacent Areas, *PhD Thesis,* Almaty, 2018.

Barbarin, B., A review of the relationships between granitoid types, their origins and their geodynamic environments, *Lithos,* 1999, vol. 46, pp. 605–626.

Beard, J.S. and Lofgren, G.E., Dehydration melting and water-saturated melting of basaltic and andesitic greenstones and amphibolites at 1, 3, and 6.9 kbar, *J. Petrol.,* 1991, vol. 32, pp. 365–401.

Beskin, S.M., Larin, V.M., and Marin, Yu.B., *Redkometall'nye granitovye formatsii* (Rare-Metal Granite Formations), Leningrad: Nauka, 1979.

Black, L.P., Kamo, S.L., Allen, C.M., et al., Improved $^{206}Pb/^{218}U$ microprobe geochronology by the monitoring of a trace-element-related matrix effect: SHRIMP, ID-TIMS, ELA-ICP-MS and oxygen isotope documentation for a series of zircon standards, *Chem. Geol.,* 2004, vol. 205, pp. 115–140.

Boynton, W.V., *Cosmochemistry of the rare earth elements: meteorite studies. rare earth element geochemistry*, Amsterdam: Elsevier, 1984.

Burmakina, G.N. and Tsygankov, A.A., Mafic microgranular enclaves in Late Paleozoic granitoids in the Burgasy quartz syenite massif, Western Transbaikalia: composition and petrogenesis, *Petrology,* 2013, vol. 21, no. 3, pp. 280–304.

Chappell, B.W. and White, A.J.R., Two contrasting granite types, *Pacific Geol.,* 1974, vol. 8, pp. 173–174.

Collins, W.J., Beams, S.D., White, A.J.R., and Chappell, B.W., Nature and origin of A-type granites with particular reference to southeastern Australia, *Contrib. Mineral. Petrol.,* 1982, vol. 80, pp. 189–200.

Cuney, M. and Barbey, P., Uranium, rare metals, and granulite-facies metamorphism, *Geosci. Front.,* 2014, vol. 5, no. 5, pp. 729–745.

Degtyarev, K.E., *Tektonicheskaya evolyutsiya rannepaleozoiskikh ostrovoduzhnykh sistem i formirovanie kontinental'noi kory kaledonid Kazakhstana* (Tectonic Evolution of the Early Paleozoic Island-Arc Systems and Formation of Continental Crust of the Kazakhstan Caledonides), Moscow: GEOS, 2012.

Degtyarev, K.E., Shatagin, K.N., Kovach, V.P., and Tret'yakov, A.A., The formation processes and isotopic structure of continental crust of the Chingiz Range Caledonides (Eastern Kazakhstan), *Geotectonics,* 2015, vol. 49, no. 6, pp. 485–514.

Dobretsov, N.L., Borisenko, A.S., Izokh, A.E., and Zhmodik, S.M., A thermochemical model of Eurasian Permo-Triassic mantle plumes as a basis for prediction and exploration for Cu–Ni–PGE and rare-metal ore deposits, *Russ. Geol. Geophys.,* 2010, vol. 51, no. 9, pp. 903–924.

Eby, G.N., Chemical subdivision of the a-type granitoids: petrogenetic and tectonic implications, *Geology,* 1992, vol. 20, pp. 641–644.

Ermolov, P.V., Izokh, E.P., Ponomareva, A.P., and Tyan, V.D., *Gabbro-granitnye serii zapadnoi chasti Zaisanskoi skladchatoi sistemy* (Gabbro-Granite Series of the Western Zaisan Orogenic System), Novosibirsk: Nauka, 1977.

Ermolov, P.V., Vladimirov, A.G., Izokh, A.E., et al., *Orogennyi magmatizm ofiolitovykh poyasov (na primere Vostochnogo Kazakhstana)* (Orogenic Magmatism of Ophiolite Belts: Evidence from the Eastern Kazakhstan), Novosibirsk: Nauka, 1983.

Frolova, O.V., Study of Geological Structure and Composition of Ores of the Verkhnee Espe Rare-Earth Deposit for Construction of Forecasting-Prospecting Model (Eastern Kazakhstan), *Extended Abstract of Doctoral (Geol.-Min.) Dissertation,* Ust'-Kamenogorsk, 2018. 145 s.

Frost, B.R., Barnes, C.G., Collins, W.J., et al., A geochemical classification for granitic rocks, *J. Petrol.,* 2001, vol. 42, pp. 2033–2048.

Frost, C.D. and Frost, B.R., On ferroan (A-type) granitoids: their compositional variability and modes of origin, *J. Petrol.,* 2011, vol. 52, no. 1, pp. 39–53.

Grebennikov A.V. A-type granites and related rocks: problems of identification, petrogenesis, and classification, *Russ. Geol. Geophys.,* 2014, vol. 55, no. 9, pp. 1074–1086.

Griffin, W.L., Powell, W.J., Pearson, N.J., and O'Reilly, S.Y., Glitter: data reduction software for laser ablation ICP-MS, *Laser Ablation ICP-MS in the Earth Sciences: Current Practices and Outstanding Issues,* Ed. Sylvester, P., Eds., *Mineral. Ass. Canada, Short Course Ser.,* 2008, vol. 40, pp. 307–311.

Khromykh, S.V., Basic and associated granitoid magmatism and geodynamic evolution of the Altai accretion–collision system (Eastern Kazakhstan), *Russ. Geol. Geophys.,* 2022, vol. 63, no. 3, pp. 279–299.

Khromykh, S.V., Tsygankov, A.A., Kotler, P.D., et al., Late Paleozoic granitoid magmatism of Eastern Kazakhstan and western Transbaikalia: plume model test, *Russ. Geol. Geophys.,* 2016, vol. 57, no. 5, pp. 773–789.

Khromykh, S.V., Kotler, P.D., and Semenova, D.V., Geochemistry, age, and geodynamic settings of the formation of the Saur gabbro-granitoid intrusive series (Eastern Kazakhstan), *Geosfer. Issled.,* 2019, no. 2, pp. 6–26.

Khromykh, S.V., Kotler, P.D., Izokh, A.E., and Kruk, N.N., A review of Early Permian (300–270 Ma) magmatism in Eastern Kazakhstan and implications for plate tectonics and plume interplay, *Geodynam. Tectonophys.,* 2019, vol. 10, no. 1, pp. 79–99.

Khromykh, S.V., Semenova, D.V., Kotler, P.D., et al., Orogenic volcanism in Eastern Kazakhstan: composition, age, and geodynamic position, *Geotectonics,* 2020, vol. 54, no. 4, pp. 510–528.

Khromykh, S.V., Kotler, P.D., Kulikova, A.V., et al., Early Triassic monzonite–granite series in Eastern Kazakhstan as a reflection of Siberian large igneous province activity, *Minerals,* 2022, vol. 12, no. 9, p. 1101.
https://doi.org/10.3390/min12091101

Khubanov, V.B., Buyantuev, M.D., and Tsygankov, A.A., U-Pb dating of zircon from Pz3–Mz igneous complexes of Transbaikalia by sector-field mass spectrometry with laser sampling: technique and comparison with SHRIMP, *Russ. Geol. Geophys.,* 2016, vol. 57, no. 1, pp. 190–205.

Kotler, P.D., Khromykh, S.V., Vladimirov, A.G., et al., New data on the age and geodynamic interpretation of the Kalba–Narym granitic batholith, Eastern Kazakhstan, *Dokl. Earth Sci.,* 2015, vol. 462, no. 5, pp. 565–569.

Kotler, P.D., Khromykh, S.V., Kruk, N.N., et al., *Granitoids of the Kalba batholith, Eastern Kazakhstan: U-Pb zircon age, petrogenesis and tectonic implications*, *Lithos,* 2021, vol. P, pp. 388–389.

Leake, B.E., Woolley, A., Charles, E.S., and Birch, W., Nomenclature of amphiboles: report of the subcommittee on amphiboles of the international mineralogical association, commission on new minerals and mineral names, *Am. Mineral.,* 1997, vol. 82, pp. 1019–1037.

Levashova, E.V., Skublov, S.G., Oitseva, T.A., et al., First age and geochemical data on zircon from riebeckite granites of the Verkhnee Espe rare earth–rare metal deposit, East Kazakhstan, *Geochem. Int.,* 2022, vol. 67, no. 1, pp. 1–15.

Li, X. and Zhang, C., Machine learning thermobarometry for biotite-bearing magmas, *J. Geophys. Res.: Solid Earth,* 2023, vol. 127. e2022JB024137.
https://doi.org/10.1029/2022JB024137

Lopatnikov, V.V., Izokh, E.P., Ermolov, P.V., et al., *Magmatizm i rudonosnost' Kalba-Narymskoi zony Vostochnogo Kazakhstana* (Magmatism and Ore Potential of the Kalba–Narym Zone of Eastern Kazakhstan), Moscow: Nauka, 1982.

Ludwig, K.R., *Isoplot 3.00: a Geochronological Toolkit for Microsoft Excel*, Berkeley: Geochronology Center, 2003.

Nikolaeva, I.V., Palessky, S.V., Chirko, O.S., and Chernonozhkin, S.M., ICP-MS determination of major and trace elements in silicate rocks after fusion with $LiBO_2$, *Analitika Kontrol'*, 2012, vol. 16, no. 2, pp. 134-142.

Patiño Douce, A.E., What do experiments tell us about the relative contributions of crust and mantle to the origin of granitic magmas? *Geol. Soc., London, Spec. Publ.,* 1999, vol. 168.

Pearce, J.A. and Norry, M.J., Petrogenetic implications of Ti, Zr, Y, and Nb variations in volcanic rocks, *Contrib. Mineral. Petrol.,* 1979, vol. 69, pp. 33–47.

Pearce, J.A., Harris, N.W., and Tindle, A.G., Trace element discrimination diagrams for the tectonic interpretation of granitic rocks, *J. Petrol.,* 1984, vol. 25, pp. 956–983.

Renna, M.R., Tribuzio, R., and Tiepolo, M., Interaction between basic and acid magmas during the latest stages of the post-collisional Variscan evolution: clues from the gabbro-granite association of Ota (Corsica–Sardinia batho-

lith), *Lithos,* 2006, vol. 90, nos. 1–2, pp. 92–110. https://doi.org/10.1016/j.lithos.2006.02.003

Reverdatto, V.V., Likhanov, I.I., Polyansky, O.P., et al., *Priroda i modeli metamorfizma* (Nature and Models of Metamorphism), Novosibirsk: SO RAN, 2017.

Rickwood, P.C., Boundary lines within petrologic diagrams which use oxides of major and minor elements, *Lithos,* 1989, vol. 22, pp. 247–263.

Rieder, M., Cavazzini, G., D'Yakonov, Y.S., et al., Nomenclature of the micas, *Can. Mineral.,* 1998, vol. 36, pp. 905–912.

Rosen, O.M. and Fedorovsky, V.S., *Kollizionnye granitoidy i rassloenie zemnoi kory (primery kainozoiskikh, paleozoiskikh i proterozoiskikh kollizionnykh sistem)* (Collisional Granitoids and Layered Earth's Crust: Evidence from Cenozoic, Paleozoic, and Proterozoic Collisional Systems), Moscow: Nauchnyi mir, 2001.

Sen, G., *Petrology. Principles and Practice,* Berlin–Heidelberg: Springer-Verlag, 2014.

Sharpenok, L.N., Kostin, A.E., Kukharenko, E.A., TAS-diagram total alkali–silica for chemical classification and identification of plutonic rocks, *Regional. Geol. Metallogen.,* 2013, no. 56, pp. 40–50.

Shcherba, G.N., D'yachkov, B.A., Nakhtigal, G.P., *Zharma-Saurskii Geotektonogen* (Zharma–Saur Geotechnogen), Alma-Ata: Nauka, 1976.

Slama, J., Kosler, J., Condond. J., et al., Plesovice zircon—a new natural reference material for u-pb and hf isotopic microanalysis, *Chem. Geol.,* 2008, vol. 249, nos. 1–2, pp. 1–35.

Steager, R.H. and Jäger, E., Subcommission on geochronology: convention on the use of decay constants in geocosmochronology, *Earth Planet. Sci. Lett.,* 1977, vol. 36, pp. 359–362.

Sun, S.-S. and McDonough, W.F., Chemical and isotopic systematics of oceanic basalts: implications for mantle composition and processes, *Geol. Soc. London: Spec. Publ.,* 1989, vol. 42, pp. 313–345.

Travin, A.V., Yudin, D.S., Vladimirov, A.G., et al., Thermochronology of the Chernorud Granulite Zone, Ol'khon Region, Western Baikal Area, *Geochem. Int.,* 2009, vol. 47, no. 11, pp. 1107–1124.

Tsygankov, A.A., Khubanov, V.B., Travin, A.V., et al., Late Paleozoic gabbroids of western Transbaikalia: U-Pb and Ar-Ar isotopic ages, composition, and petrogenesis, *Russ. Geol. Geophys.,* 2016, vol. 57, no. 5, pp. 790–808.

Tsygankov, A.A., Khubanov, V.B., Udoratina, O.V., et al., Alkaline granitic magmatism of the western Transbaikalia: petrogenetic and geodynamic implications from U-Pb isotopic-geochronological data, *Lithos,* 2021, vol. 390-391, p. 106098.

Vielzeuf, D. and Montel, J.M., Partial melting of metagreywackes. Part I. Fluid-absent experiments and phase relationships, *Contrib. Mineral. Petrol.,* 1994, vol. 117, pp. 375–393.

Vladimirov, A.G., Kruk, N.N., Khromykh, S.V., et al., Permian magmatism and lithospheric deformation in the Altai caused by crustal and mantle thermal processes, *Russ. Geol. Geophys.,* 2008, vol. 49, no. 7, pp. 468–479.

Whalen, J.B., Currie, K.L., and Chappell, B.W., A-type granites: geochemical characteristics, discrimination and petrogenesis, *Contrib. Mineral. Petrol.,* 1987, vol. 95, pp. 407–419.

Xu, Y-G., Wei, X., Luo, Z-Y., et al., The early permian tarim large igneous province: main characteristics and a plume incubation model, *Lithos,* 2014, vol. 204, pp. 20–35.

Yarmolyuk V.V., Kozlovsky, A.M., and Kuzmin, M.I., Zoned magmatic areas and anorogenic batholith formation in the Central Asian Orogenic Belt (by the example of the Late Paleozoic Khangai magmatic area), *Russ. Geol. Geophys.,* 2016a, vol. 57, no. 3, pp. 357–370.

Yarmolyuk, V.V., Kozlovsky, A.M., Savatenkov, V.M., et al., Composition, sources, and geodynamic nature of giant batholiths in Central Asia: evidence from the geochemistry and Nd isotopic characteristics of granitoids in the Khangai zonal magmatic area, *Petrology,* 2016b, vol. 24, no. 5, pp. 433–461.

Yarmolyuk, V.V., Kuzmin, M.I., and Ernst, R.E., Intraplate geodynamics and magmatism in the evolution of the Central Asian Orogenic Belt, *J. Asian Earth Sci.,* 2014, vol. 93, pp. 158–179.

Zonenshain, L.P., Kuzmin, M.I., and Natapov, L.M., *Tektonika litosfernykh plit territorii SSSR* (Tectonics of Lithosphere Plates of the USSR Territory), Moscow: Nedra, 1990.

Translated by M. Bogina